KfK 4404
September 1988

Out-of-pile Experiments on LWR Severe Fuel Damage Behavior

Tests CORA-C and CORA-2

S. Hagen, L. Sepold, P. Hofmann, G. Schanz
Hauptabteilung Ingenieurtechnik
Institut für Material- und Festkörperforschung
Projektgruppe LWR-Sicherheit

Kernforschungszentrum Karlsruhe

KERNFORSCHUNGSZENTRUM KARLSRUHE

Hauptabteilung Ingenieurtechnik

Institut für Material- und Festkörperforschung

Projektgruppe LWR-Sicherheit

KfK 4404

Out-of-pile Experiments on LWR Severe Fuel Damage Behavior

(Tests CORA-C and CORA-2)

S. Hagen, L. Sepold,

P. Hofmann, G. Schanz

Kernforschungszentrum Karlsruhe GmbH, Karlsruhe

Als Manuskript vervielfältigt
Für diesen Bericht behalten wir uns alle Rechte vor

Kernforschungszentrum Karlsruhe GmbH
Postfach 3640, 7500 Karlsruhe 1

ISSN 0303-4003

Abstract

The out-of-pile experiments of the CORA program performed within the LWR Safety Project (PRS) at the Kernforschungszentrum Karlsruhe (KfK) are to provide information on the damage mechanisms of LWR fuel elements under severe fuel damage (SFD) conditions, i.e. in the temperature region from 1200°C to above 2000°C. In these experiments the decay heat is simulated by electrical heating of a central tungsten rod within annular pellets, which are placed inside the Zircaloy-4 (Zry) cladding. The test bundle in the CORA-facility is arranged from 16 heated (1000 mm length) and 9 unheated rods (full pellets) surrounded by a Zry shroud. The shroud itself is insulated by ZrO_2 fiber insulation to obtain a uniform radial temperature distribution. In the test program 15 experiments are planned, five experiments have been performed (by May 1988). In this paper the results of one of two tests with Al_2O_3 pellets and one of two tests with UO_2 pellets (spacer of Inconel, no absorber material present) are reported.

In the tests with Al_2O_3 pellets, simulating burnable poison rods (98.6 wt.% Al_2O_3 + 1.4 wt.% B_4C), early melt formation at about 1350°C was observed. The liquefaction increases distinctly at 1500°C. In the resolidified melts two metallic phases: α-Zr(O) and (Zr, Al) alloy and one porous ceramic (ZrO_2/Al_2O_3) eutectic can be distinguished. Large blockages form at the lower end of the bundle. In the tests with UO_2 pellets the melting starts at the elevation of the Inconel grid spacer. By eutectic melt formation in contact with the zircaloy the liquefaction begins already below the melting point of the Zry and Inconel. Further interaction of this melt with the UO_2 results in partial dissolution of the pellets. Solidification of the melt led to blockage formation at the lower end of the bundle, but at higher elevations compared to the tests with alumina pellets. At some locations fragmentation of fuel pellets to fine powder took place during cooldown.

This report is an extended version of a presentation held at the "International Symposium on Severe Accidents in Nuclear Power Plants" in Sorrento (Italy), March 1988.

Out-of-pile Experimente zur Untersuchung schwerer Kernschäden an Leichtwasser-Reaktoren (Versuche CORA-C und CORA-2)

Die out-of-pile Experimente des CORA-Programms werden im Rahmen der Projektgruppe LWR Sicherheit (PRS) durchgeführt. Sie sollen Informationen über die Schadensmechanismen an LWR-Brennelementen im Temperaturbereich von 1200°C bis jenseits 2000°C liefern.
Die Nachwärme wird in diesen Experimenten durch das elektrische Aufheizen von Wolfram-Stäben simuliert. Der Heizstab ist von Ringpellets umgeben, die von einem Zircaloy-4 (Zry)-Hüllrohr umgeben sind. Das Testbündel der CORA-Anlage ist aus 16 beheizten und 9 unbeheizten Stäben aufgebaut. Es wird von einem Zry-Dampfführungsrohr umgeben. Dieses wiederum ist durch eine ZrO_2-Faserschicht isoliert, um eine möglichst gleichmäßige radiale Temperaturverteilung zu erhalten.
In der Testmatrix des CORA-Programms sind ca. 15 Experimente geplant. Fünf Experimente wurden bisher durchgeführt (Mai 1988). In diesem KfK-Bericht wird über den Versuch CORA-C mit Al_2O_3-Pellets und den Versuch CORA-2 mit UO_2-Pellets berichtet.

In dem Experiment mit Al_2O_3-Pellets, das das Verhalten von abbrennbaren Neutronenabsorberstäben simulieren sollte (98.6 Gew.% Al_2O_3 und 1.4 Gew.% B_4C), wurde die erste Schmelze schon ab 1350°C bemerkt. Die Verflüssigung der Stäbe nahm bei 1500°C deutlich zu. In den erstarrten Schmelzmassen kann man zwei metallische Phasen [α-Zr(O) und eine (Zr, Al) Legierung] und eine poröse keramische Phase (ZrO_2/Al_2O_3-Eutektikum) finden. Am unteren Ende des Bündels haben sich starke Blockaden ausgebildet.

Im UO_2-Test begannen die Schmelzerscheinungen auf der Höhe des Inconel-Abstandshalters. Durch eutektische Schmelzbildung am Kontakt zwischen Inconel und Zry begann die Verflüssigung schon unterhalb der Schmelztemperatur des Zry-Hüllmaterials und Abstandshalters. Die daraus folgende Wechselwirkung dieser Schmelze mit dem UO_2 führte zum Auflösen der Pellets und zur Bildung einer uranhaltigen Schmelze. Das Erstarren der Schmelze führte zur Blockadenbildung am unteren Ende des Bündels, aber in einer Höhe, die deutlich über derjenigen des Al_2O_3 Bündels lag. An einigen Positionen des CORA-2-Bündels kann man die

Fragmentierung der UO_2-Pellets während des Abkühlens bis hin zu feinem Pulver erkennen.

Dieser Bericht ist eine erweiterte Fassung eines Vortrags der auf dem "International Symposium on Severe Accidents in Nuclear Power Plants" in Sorrento (Italien) im März 1988 gehalten wurde.

Contents

1. INTRODUCTION

The TMI-2 accident has demonstrated that a severe fuel damage transient will not necessarily escalate to an uncontrolled core meltdown accident, if the design basis accident limits are exceeded. Therefore, comprehensive research programs have been initiated in various countries to investigate the relevant damage mechanisms and furthermore the margin of safety.

In the Federal Republic of Germany at the Kernforschungszentrum Karlsruhe (KfK) the Severe Fuel Damage (SFD) Program [1] was coordinated by the Project Nuclear Safety (PNS), now Project Group LWR Safety (PRS). In the CORA Program [2], which is an important part of this effort, out-of-pile experiments are performed to provide information on the behavior of Light Water Reactor (LWR) fuel elements under severe fuel damage (SFD) conditions.

According to the present knowledge the most important aspects are the formation of liquid phases by interaction between the Zircaloy-4 (Zry) cladding and the UO_2 pellets in competition to the oxidation of the cladding by steam. The chemical behavior of the fuel rods is influenced by the interaction with grid spacers, absorber rods, guide tubes, and burnable poison rods. In addition, fragmentation of fuel elements during reflooding will be investigated.

For the experimental approach at KfK two facilities are being used: (1) the NIELS facility which has been in operation for several years, and (2) the CORA facility which was especially designed for the SFD experiments. In both facilities the decay heat of the fuel rods is simulated by electrical heating using central tungsten heaters. In the CORA test program a total of 15 experiments with UO_2 pellets are planned. Up to now (May 1988) two tests with Al_2O_3, simulating burnable poison rod material, and three tests with UO_2 pellets have been performed in the CORA facility (see Table 1).

The NIELS experiments have served as CORA scoping tests to a certain extent. Results of the NIELS tests have been reported previously. A brief summary of results from the various test series is given in the following section.

The main emphasis within the SFD experimental work at KfK is now on the CORA experiments.

In this report first results from two CORA experiments, i.e. Al_2O_3 test CORA-C and UO_2 test CORA-2, are discussed. Detailed information on tests CORA-C and CORA-2 will be published with References [4, 6] and [5, 7], respectively.

Table: 1 CORA experiments performed (status May 1988)

Test No.	Max. cladding temperatures	Absorber material	Other test conditions	Date of test
B	≈ 2000°C	-	Ar + steam atmosphere, Al_2O_3 pellets	Sept. 3, 1986
C	≈ 2000°C	-	Al_2O_3 pellets	Feb. 2, 1987
2	≈ 2000°C	-	UO_2 pellets, Inconel spacer	Aug. 6, 1987
3	≈ 2400°C	-	UO_2 pellets, Inconel spacer High temp.	Dec. 3, 1987
5	≈ 2000°C	Ag, In, Cd		Feb. 26, 1988

2. NIELS RESULTS

The experiments carried out in the NIELS facility (single rods and 3x3 bundles) were to investigate the basic phenomena of fuel rod damage under temperature escalations. So, a variety of tests were performed to study the temperature escalation behavior of Zry fuel rods in steam environments. Furthermore, the interaction between Zry and UO_2, or Inconel grid spacers, guide tubes (Zry or stainless steel) and absorber rods were investigated [3].

Single rod tests on the temperature escalation behavior showed that the temperature escalation due to the exothermal Zry/steam reaction depends on the initial heatup rate which determines the thickness of the oxide layer, and has a decisive influence on the damage initiation of the fuel rod. The external oxidation of the cladding by steam competes with the chemical interactions between the cladding and the fuel.

3x3 bundle tests with (Ag, In, Cd) absorber rods showed that the failure temperature of the absorber rod cladding is dependent on the guide tube material. Absorber rods with Zry guide tubes failed at about 1200°C and absorber rods with stainless steel guide tubes failed at about 1350°C (Table 2).

Table 2: Failure temperatures of (Ag,InCd) absorber rods in the 3x3 array of the NIELS test apparatus

Test	Max. Temp. within bundle	Failure temp.	Absorber rod cladding	Guide tube material	Grid spacer material
ABS-4	1170°C	No failure	SS	Zry	Inc.
ABS-3	1400°C	1200°C	SS	Zry	Inc.
ABS-2	1850°C	1200°C	SS	Zry	Inc.
ABS-1	2050°C	1200°C	SS	Zry	Inc.
ABS-6	1400°C	1350°C	SS	SS	Inc.

SS = Stainless steel
Zry = Zircaloy-4
Inc. = Inconel 718

In tests with B_4C absorber material failure of the absorber rod occurred at about 1200°C. The resulting liquid B_4C/stainless steel interaction products cause failure of the fuel rods below the melting points of the individual components.

3. CORA FACILITY

A schematic view of the CORA facility [2] is given in Fig. 1 and a schematic of the test section, i.e. the bundle inside the high-temperature shield, is provided with Fig. 2. A 25-rod bundle with an overall length of 2 m and a heated length of 1 m is being used in the test section of the facility. The bundle consists of 16 heated and 9 unheated rods (Fig. 2). The design characteristics of the heated and unheated fuel rod simulator are depicted in Fig. 3 and are listed in more detail in Table 3. In the heated rod the centrally located tungsten heater of 6 mm diameter is surrounded by annular Al_2O_3 pellets (Tests CORA-B and CORA-C) or annular UO_2 pellets (CORA-2, CORA-3, and future CORA-tests) inside the Zry cladding which is identical to that used in Pressurized Water Reactors (PWR). The unheated rod consists of annular Al_2O_3 pellets and of full UO_2 pellets respectively, in Zry tubing. Three spacers are positioned at the bottom, the center, and at a top elevation (Table 3). In the Al_2O_3 tests Zry is used for all spacers, but in the UO_2 tests an Inconel spacer is used at the middle elevation. The bundle is surrounded by a 1-mm thick zircaloy shroud within a 20-mm ZrO_2 fiber insulation. This insulation guarantees a uniform radial temperature distribution across the bundle.

The temperatures of the test section are measured with W/Re and NiCr/Ni thermocouples and by two-color pyrometers.

The CORA facility has the following improvements compared to the smaller NIELS facility: Larger bundles (max. 7x7) and longer bundles (2 m overall length) can be used. To investigate the influence of ballooning of the cladding on the SFD initiation and propagation, the fuel rod simulators can be internally pressurized up to 100 bar.
A system pressure of 10 bar maximum can also be applied. To study the fragmentation of embrittled bundles caused by quenching, the bundle can be flooded with water from the bottom. During the test, the damage progression in the bundle at selected elevations is registered by video systems and 35-mm still cameras. After the test, the bundle can be inspected and photographed without any mechanical handling of the bundle.

Table 3: Design characteristics of the fuel rod simulators used in tests CORA-C and CORA-2

Rod outside diameter:				10.75 mm
Cladding material:				Zircaloy-4
Cladding thickness:				0.725 mm
Rod length:				2175 mm
Heated length:				1000 mm
Bundle size:				25 rods
Number of heated rods:				16
Fuel simulator	heated rods:	CORA-C		Al_2O_3 annular pellets
		CORA-2		UO_2 annular pellets
	unheated rods:	CORA-C		Al_2O_3 annular pellets
		CORA-2		UO_2 solid pellets
Heater material:				Tungsten
Heater diameter:			6 mm	
Pitch:				14.3 mm
Grid spacer	- Material:			Zircaloy-4, Inconel
	- Length:	Zry-4:		42 mm
		Inconel:		38 mm
	- Axial location:	CORA-C	lower:	-5 mm [(a)]
			center:	500 mm
			top:	938 mm
	- Axial location	CORA-2:	lower:	-5 mm
			center:	488 mm
			top:	880 mm
Shroud:	- Material:			Zircaloy-4
	- Wall thickness:			1 mm
	- Outside dimensions:			86 x 86 mm
	- Elevation:			36-1241 mm
Shroud insulation:				
	- Material:			ZrO_2
	- Thickness			20 mm

(a) Elevations are meant for the top of the grid spacer and are referred to the bottom of the heated zone (0 mm = EL 5121).

4. TEST CONDUCT

Three periods can be distinguished in the test sequence of the CORA experiments: For the first 3000 s pre-heated argon of about 600°C enters the bundle with a flow rate of 5 g/s. Between 3000 s and 4800 s the electric power is increased from 6 kW to 30 kW (Fig. 4) to achieve the target heatup rate of 1 K/s. At 3300 s within the test a constant (superheated) steam flow of 5 g/s is added to the argon flow. The test is terminated by reduction of electric power.

After the visual inspection of the damaged bundle it is fixed by embedding in epoxy for sectioning it and preparing it for the metallographic investigation, which is described in section 6.

5. CORA-EXPERIMENTAL RESULTS

5.1 Tests with Al_2O_3 Pellets

5.1.1 Temperature Response

To generate the temperature transient in test CORA-C an electric power input as given in lower part of Fig. 4 was used. The temperature responses of unheated rods at different axial elevations are given in the upper part of this figure. For the first 1000 sec the temperature is increasing nearly linearly. Due to the steam and gas entering at the lower end of the bundle higher temperatures have developed in the upper half compared to the lower half of the symmetrically built bundle.

A temperature escalation due to the exothermal Zry/steam reaction is first observed at the 550 mm elevation. The onset of the escalation is influenced by the competition between the energy gain due to the exothermal reaction and the energy losses. In the CORA arrangement the heat losses are kept small by the ZrO_2 fiber insulation around the shroud leading to an early start of the temperature increase.

The escalations in the upper and lower part of the bundle are less pronounced or develop at a later time. They are triggered by the heat transport from the much hotter axial middle region to the upper part by convection and to the lower region by the melt running down.

5.1.2 Videoscope Inspection

To investigate the time-dependent behavior of the bundle 10 videoscopes were aimed at windows in the shroud insulation. The recording is performed by videocameras and 35-mm still cameras. The first movement of melt during test CORA-C was registered at 4150 s and at 400 mm (see Fig. 5 at 300 mm). The melt was dropping down from higher elevations. Fig. 4 explains that at this time a temperature of about 1400°C was reached at 550 mm. Exceeding 1500°C the melt formation was drastically increasing. This early melt formation in simulators which contain only Zry and Al_2O_3 (only Zry grid spacers were used in this test) is therefore clearly caused by the chemical interaction between Zry and Al_2O_3.

5.1.3 Post-test Appearance of the Al_2O_3/Zr Bundle

The post test appearance of CORA-C is demonstrated in Fig. 6. The photograph shows the bundle within the shroud (at different orientations) after lowering the high temperature shield and removing the fiber insulation. Most of the shroud was still intact, but was heavily deformed and embrittled. The largest shroud deformation occurred in the region between 300 mm and 700 mm, i.e. in the region of the axial peak temperature. Fig. 7 gives details of the region 250-430 mm. The deformation is more pronounced in the lower part of the bundle (below about 650 mm elevation). The upper part (Fig. 8, 770-930 mm) exhibits intact pellets with a cladding broken off due to embrittlement. An enhanced interaction zone lies between 600 and 700 mm (Fig. 9, 610-800 mm).
Complete dissolution of the Al_2O_3 pellets by molten Zry can be found up to about 650 mm elevation. Above this elevation more and more remnants of the Al_2O_3 pellets are present.
Fig. 10 shows the lower end of the bundle above about 100 mm elevation after removal of the shroud. Here the fuel rod simulators have completely melted away. Only the tungsten heaters are left.

Examples of the horizontal and vertical cross sections of the bundle are given in Figs. 11 through 13. They show that a blockage has formed below about 100 mm. The amount of blockage decreases at lower elevations. At the upper end of the lower grid spacer (-5 mm elevation) only about 20% of the bundle cross section is blocked (Fig. 14). This shows the tendency of the melt to solidify between the fuel rods provided the temperature is low enough.

5.2 Tests with UO_2 Pellets

5.2.1 Temperature Response

The time dependency of the temperature in test CORA-2 is very similar to the temperature behavior in test CORA-C as is demonstrated with the radial temperature distributions in Fig. 4. For two elevations (950 and 550 mm) the temperatures for the heated rod, unheated rod, "gas" (atmosphere), outside of the shroud, and outside of the fiber insulation are given.

In the beginning of the transient the temperature traces are clearly separated decreasing from heated rod to gas, unheated rod, and shroud . The temperature on the surface of the shroud insulation is distinctly lower, a consequence of the properties of the 20 mm fiber insulation. Due to the exothermal heat from the Zry/steam reaction, which is acting on heated rods, unheated rods, and the shroud above 1000°C, the temperature curves come closer together. This flat radial temperature profile shows the good simulation quality of the fuel rod simulators with solid pellets.

At 950 mm the comparison of the temperatures of gas and heated rod shows, that in the beginning the gas temperature is clearly lower. Due to the fast temperature increase in the middle axial region by the exothermal reaction at about 4000 s the convective energy transport from the middle to the upper region is also growing. In consequence, the gas temperature at 950 mm is increasing faster, which again influences the temperature of the heated rod. Calculations of the temperature response with the SCDAP (Severe Core Damage Analysis Package) are given in [8].

5.2.2 Videoscope Inspection

Movement of melt was visible by videoscope inspection only in the lower half of the bundle below the Inconel grid spacer. The video films clearly show that the melt formation starts at the contact between Zry cladding and Inconel grid spacer (Fig. 15). This is caused by the eutectic alloy formation between the Fe, Cr and Ni of the spacer with the Zr of the fuel rod cladding.

5.2.3 Post-test Appearance of the UO_2/Zry Bundle

A photograph on the overall appearance of the bundle after test CORA-2 is given in Fig. 16. Fig. 17 shows the lower end of the bundle with the shroud removed. A large amount of refrozen melt can be seen. The melt formation started by interaction between the Inconel spacer and Zry. Uranium found in the refrozen melt proves that the liquefied Zry in contact with the pellet started to dissolve the UO_2 [9].

Lying loosely on top of refrozen melt one can recognize powdered UO_2. The fact that these fragments are not dissolved in the melt indicates that they must have formed after refreezing of the melt.

The horizontal cross sections between 253 and 300 mm elevation (Fig. 18) show that the region up to 300 mm is nearly completely blocked with refrozen melt. In the cross section at 253 mm a strong powdering of the pellets can also be recognized. The vertical cross section in Fig. 19 points out, that the melt is refrozen down to between 210 and 140 mm elevation and that above the solid blockage more loosely packed fragments have collected. The horizontal cross sections above 365 mm elevation (Fig. 20) show fewer fragments sticking between the fuel rod simulators but a clear attack of the melt on the pellets.

6. Destructive Metallographic Post-test Investigations

After the CORA tests, extensive destructive post-test examinations have been performed to determine the complex material behavior. The high temperatures reached in the CORA tests cause a variety of physical changes in the bundle material and cause various chemical interactions resulting in solid and liquid reaction products. These phenomena include phase transformations, steam oxidation of zircaloy, melting of cladding and burnable poison rod material (Al_2O_3 + 1.4 wt.% B_4C), ZrO_2, Al_2O_3 and/or UO_2 dissolution, and solidification of melts with the formation of typical microstructures. Since most of the phenomena leave characteristic patterns in the resulting microstructures and distribution of the various phases, the microstructure can be used to explain the interaction processes and to make statements concerning the maximum temperatures reached during the test. Of special concern is the formation of liquid phases which may relocate and form coolant channel blockages.

Fig. 21 shows some typical details of the cross-section elevation C7 (71 mm) of the CORA test C. The initial arrangement of the rods can still be recognized. Beside the tungsten heater, Al_2O_3 pellet and zircaloy cladding, which have been chemically attacked and/or are partially molten, one can recognize different relocated materials which solidified at this elevation and formed local blockages. In general, one can distinguish three different types of once-molten material: ceramic material which is very porous (foam-like) after solidification and consists of an eutectic mixture of the ceramic phases Al_2O_3 and ZrO_2 together with different amounts of primary Al_2O_3 and ZrO_2 constituents, a metallic (Zr,Al,O,Sn) alloy which decomposes on cooldown into α-Zr(O) and a (Zr,Al,Sn) alloy, and molten zircaloy cladding of various oxygen contents. The ceramic Al_2O_3/ZrO_2 eutectic will be liquid above about 1850 °C, the metallic (Zr,Al,Sn,O) alloy can be liquid already at about 1350 °C, and the as-received (oxygen-poor) Zircaloy cladding will melt above 1760 °C. The low-temperature melting of some of the reaction products is in agreement with the video information obtained during the tests, where first liquid phases were observed around 1400 °C.

In Fig. 21 position 1 shows the decomposed metallic (Zr,Al,Sn,O) alloy, position 2 shows the interaction of the ceramic Al_2O_3/ZrO_2 melt with an Al_2O_3 pellet where the cladding has been melted away, and position 3 shows the dissolution of an Al_2O_3 pellet by molten zircaloy cladding. The ceramic melt which is attached to the partially oxidized cladding apparently solidified rather quickly at this elevation since no pronounced interactions have taken place with the cladding. Also recognizable are the large cavities in the once molten cladding which had formed due to relocation of the liquid zircaloy. The run-off of the cladding was partially prevented by the ZrO_2 shell which formed on the cladding outer surface as a result of the interaction with steam. A detailed description of the reaction mechanisms and reaction kinetics between Al_2O_3 and zircaloy is given in [6].

Fig. 22 shows a CORA-2 bundle cross section through the blockage region at the 268 mm elevation. A metallic (Zr, U, O) melt has formed in the upper elevations which relocated and solidified in the lower part of the bundle as a result of the axial temperature gradient. At position 2 of Fig. 22 one can recognize that the cladding has disappeared and the UO_2 fuel has been chemically dissolved to different extents by the metallic melt. Strong crack pattern form in the UO_2 pellets which are the reasons for the formation of small pellet fragments and UO_2 powder which can be seen in regions where the external support of pellets by cladding is lost. The rubble is partially collected on top of the solidified melts as shown at position 3 of Figure 22. Position 1 of Fig. 22 shows the typical formation of voids between the cladding external oxide layer and the fuel pellet due to relocation of the molten metallic part of the cladding.

7. Summary and Conclusions

- The first bundle tests in the CORA facility have demonstrated its capability to simulate reactor core degradation of severe LWR accidents.

- Temperature escalation, caused by the exothermal Zry-steam reaction, starts from the initally hottest upper half of the bundle and is later locally triggered by hot steam or relocated melt.

- In the tests with Al_2O_3 pellets, simulating burnable poison rods, early melt formation and fast relocation were observed.

- The liquefaction starts at about 1350°C and increases remarkably after reaching 1500°C. The formation of a metallic (Zr, Al, O) alloy is important in this process.

- From the solidified material one can distinguish three different types of once molten material: a metallic (Zr, Al, O) alloy, metallic molten Zry of different oxygen content, and a ceramic (ZrO_2/Al_2O_3) mixture. The (Zr, Al, O) alloy can be liquid already at about 1350°C, the oxygen-poor Zr will melt above 1760°C and the ceramic Al_2O_3/ZrO_3 eutectic will be liquid above about 1850°C.

- Large blockages were formed by the refrozen melt at the lower end of the bundle. The refrozen melt is covered by rubble, i.e. by pieces from embrittled cladding and fractured pellets.

- The melt formation from burnable poison rod failure may cause additional fuel liquefaction in the respective fuel element.

- In the tests with UO_2 pellets the melting started at the elevation of the Inconel spacer. By eutectic melt formation in contact with Zry the liquefaction begins already below the melting point of the Inconel.

- Further interaction of this melt with the UO_2 results in partial dissolution of the pellets even below the Zry melting point.

- Refreezing of the melt led to blockage formations at the lower end of the bundle. This blockage in the UO_2 test developed at higher elevations (below 350 mm) compared to the experiment with Al_2O_3 pellets (below 100 mm).

- In the UO_2 test fragmentation of fuel pellets to fine powder took place during cool-down.

8. FUTURE TESTS

As described above the first CORA experiments were run without absorber materials; therefore, they can serve as reference tests. In the future CORA tests either (Ag, In, Cd) or B_4C will be inserted in the bundle. Furthermore quenching, internal rod pressure, and system pressure will be applied as test parameters.

9. ACKNOWLEDGEMENTS

Various kinds of support of the experimental program and its evaluation is gratefully acknowledged.

The test rods were assembled by Mr. E. Mackert, as were the test bundles by Messrs. H. Giesmann and Ph. Pfann. The authors would like to thank Messrs. K. Vogel, H. Benz, O. Heil, W. Rötzel, and H.J. Röhling for the preparations of the test and for the test conduct. Messrs. H. Malauschek and K.P. Wallenfels are acknowledged for arrangement of camera and video systems to observe the bundle behaviour during the transient test. Mr. W. Rötzel's effort in the post-test photography is greatly appreciated. A special acknowledgement is due to Mr. H. Benz for the encapsulation procedure of the tested bundle. The authors thank Mr. L. Anselment for the sectioning of the bundle and for the preparation of the metallographic samples, Mr. H. Metzger for the investigation of the metallographic samples by optical microscope, Mr. J. Burbach for the SEM investigation, and Mrs. B. Bennek-Kammerichs for a contribution to the microstructural investigation.

10. REFERENCES

[1] FIEGE, A.; Severe Fuel Damage Investigations of KfK/PNS, KfK 3431B, 1983

[2] HAGEN, S., HAIN, K.; Out-of-pile Bundle Experiments on Severe Fuel Damage; CORA-Program, KfK 3677, 1986

[3] HAGEN, S., HOFMANN, P.; Physical and Chemical Behaviour of LWR Fuel Elements up to very High Temperatures, KfK 4104, 1987

[4] HAGEN, S., HERING, W., VOGEL, K.; CORA-Scoping Test C, Test Results Report, KfK 4312, 1988

[5] HAGEN, S., HERING, W., VOGEL, K.; CORA-2; Test Results Report, KfK 4342, 1988

[6] HAGEN, S., HOFMANN, P., SCHANZ, G., SEPOLD, L.; Interaction between Zry-cladding and Al_2O_3-pellets, Post Test Results of Test CORA-B and CORA-C, KfK 4313, 1988

[7] HAGEN, S., HOFMANN, P., SCHANZ, G., SEPOLD, L.; Interactions in Zry/UO_2 Fuel Rod Simulator Bundles with Inconel Spacers at High Temperatures; Post Test Results of Test CORA-2 and CORA-3, KfK 4378, 1988

[8] HERING, W., MEYDER, R.; Evaluation of CORA-Experiments using SCDAP, IAEA-SM-296/31, International Symposium on Severe Accidents in Nuclear Power Plants, Sorrento (Italy), 21-25 March 1988.

[9] HOFMANN, P., UETSUKA, H., WILHELM, A.N., GARCIA, E.A.; Dissolution of solid UO_2 by molten Zry and its modelling, IAEA-SM-296/1, International Symposium on Severe Accidents in Nuclear Power Plants, Sorrento (Italy), 21-25 March 1988.

11. List of Figures

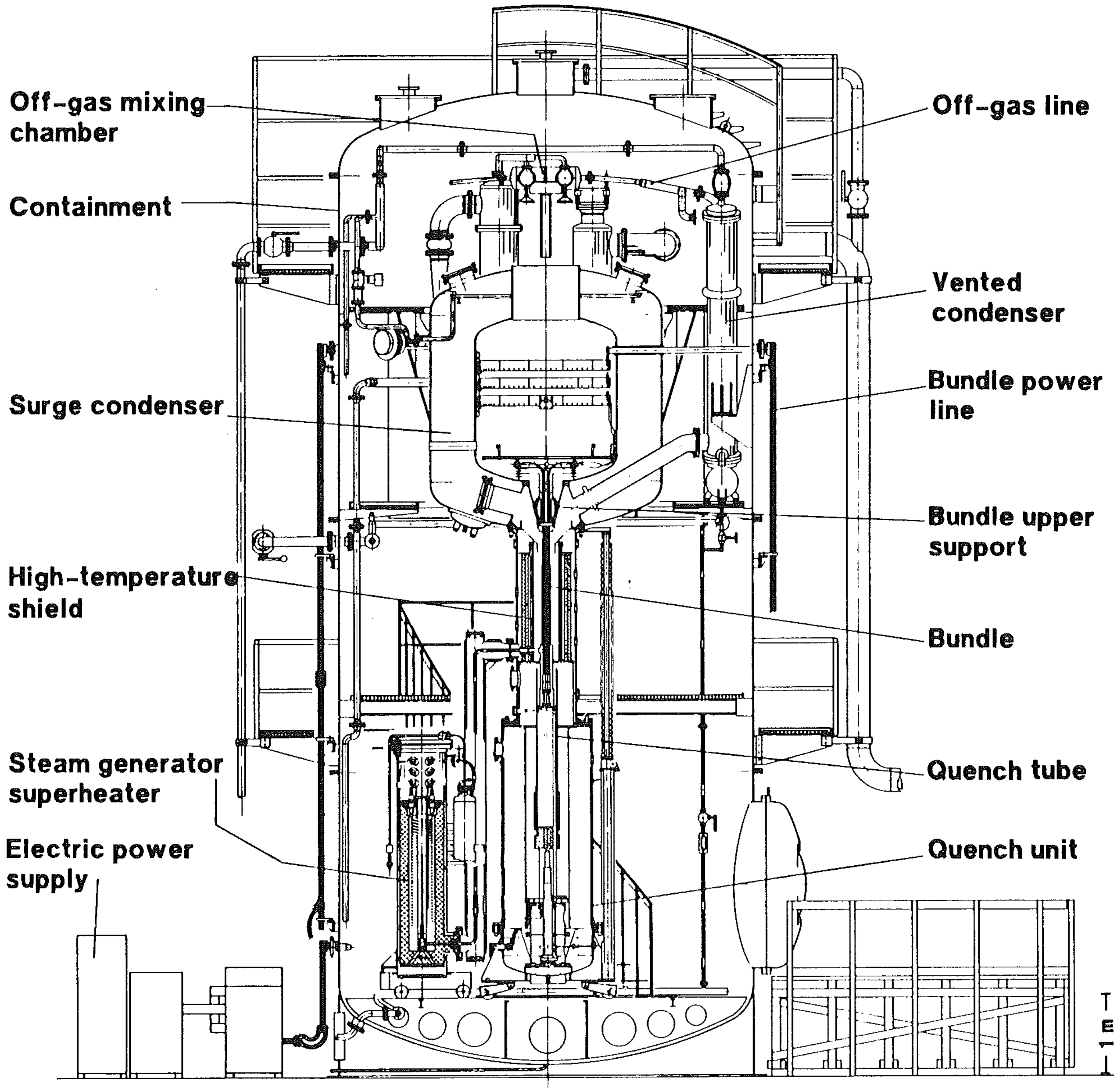

Fig. 1: SFD test facility CORA

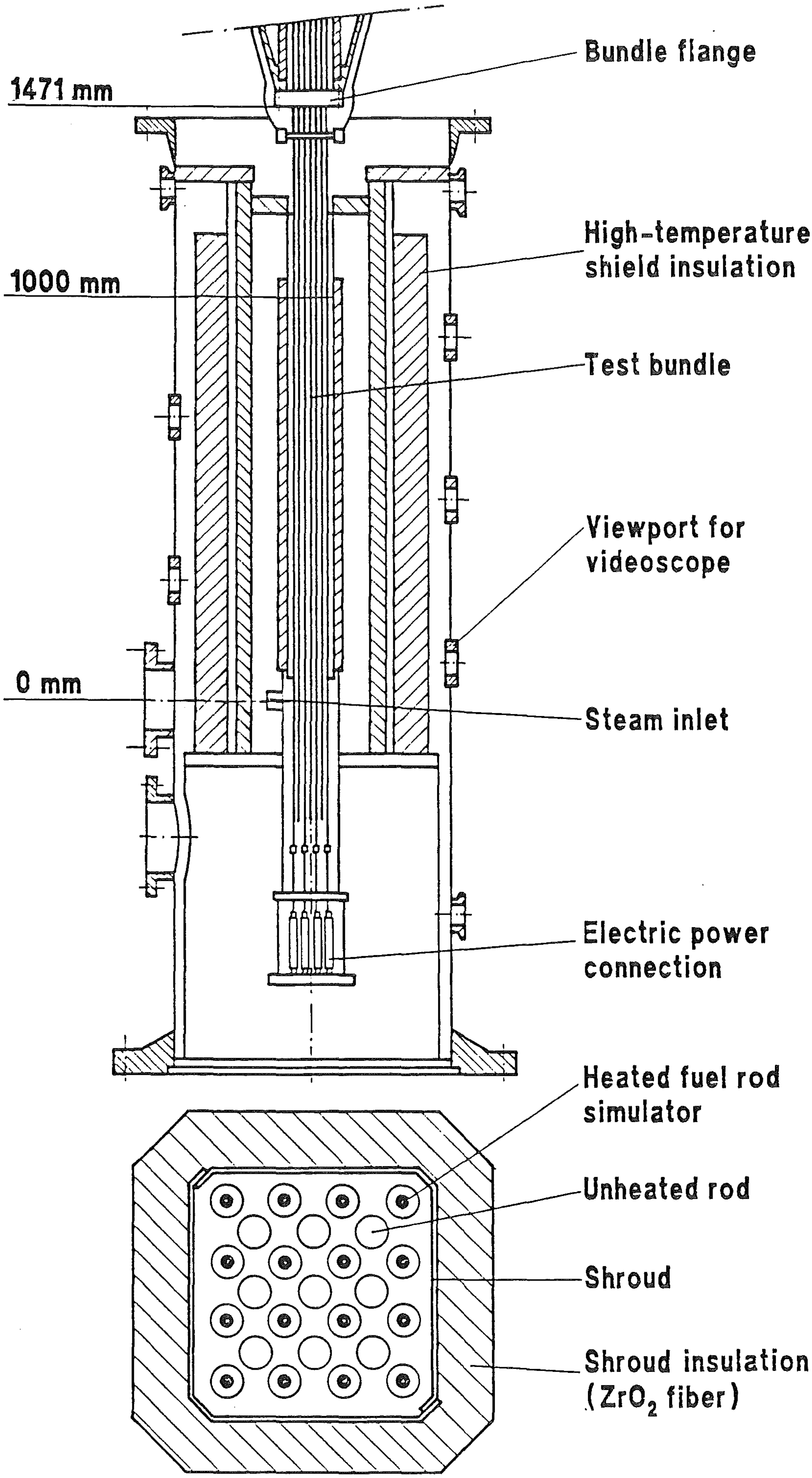

Fig. 2: CORA test section

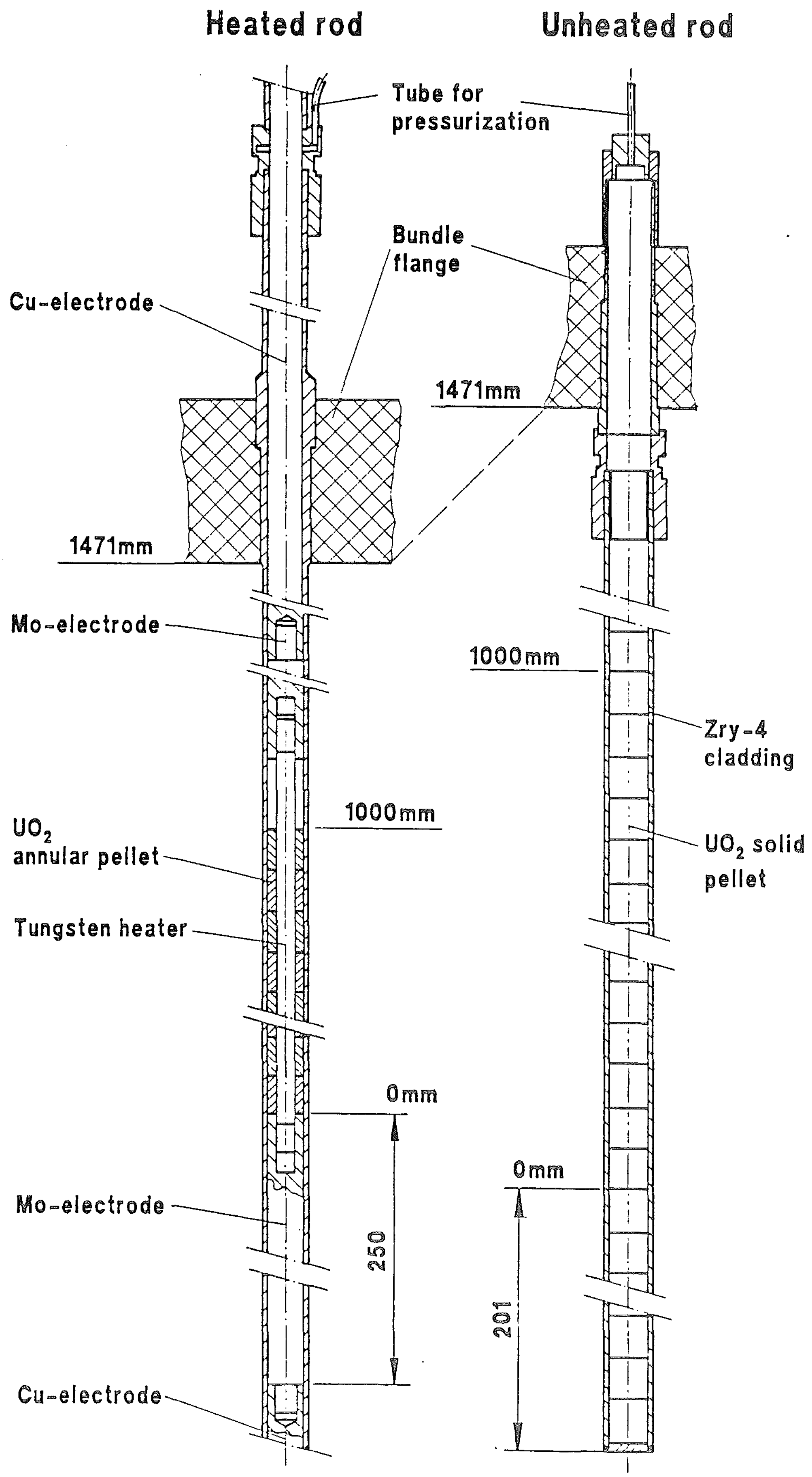

Fig. 3: Design characteristics of the CORA fuel rod simulators

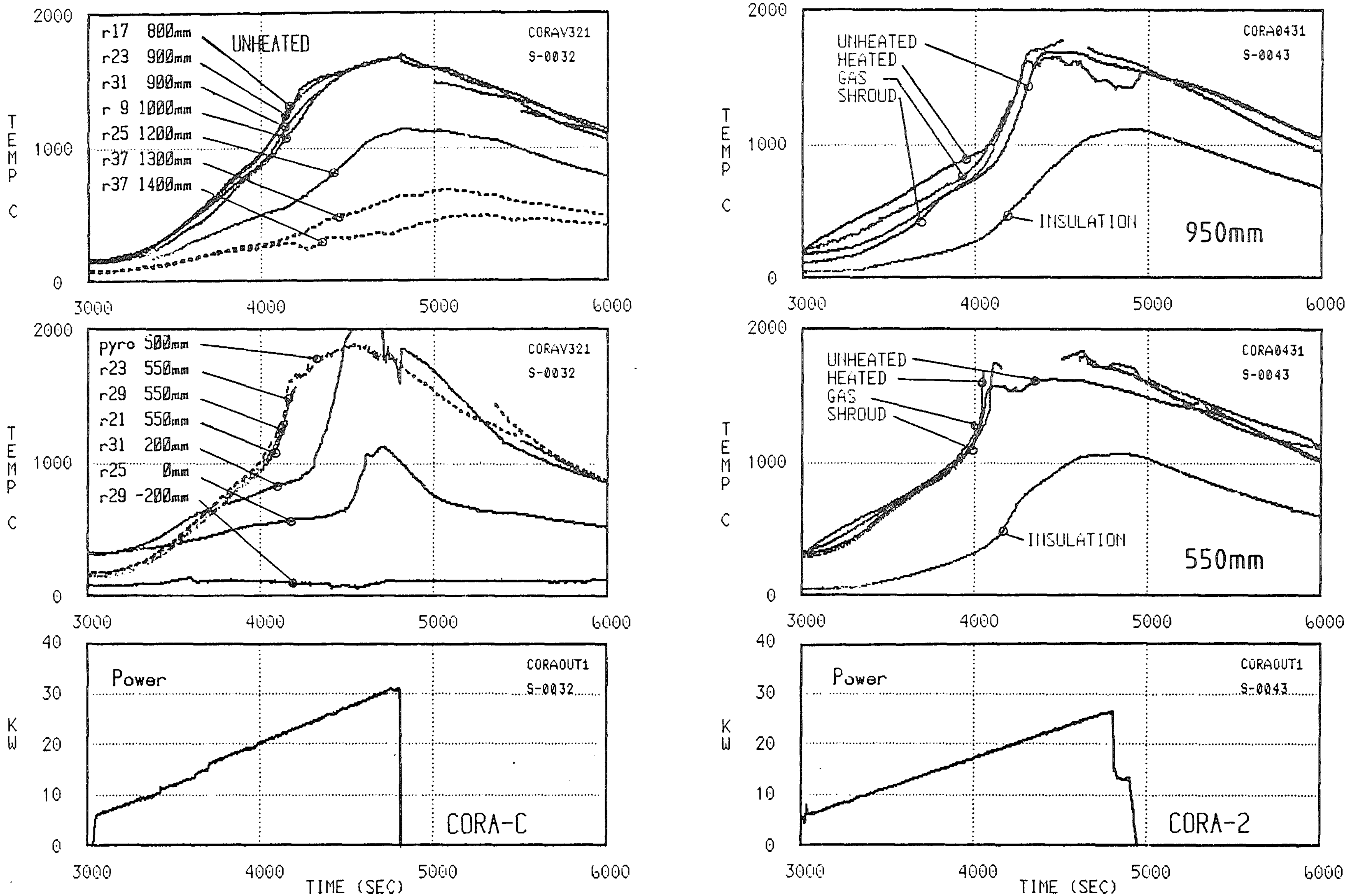

Fig. 4: Electric power input and temperatures for tests CORA-C and CORA-2

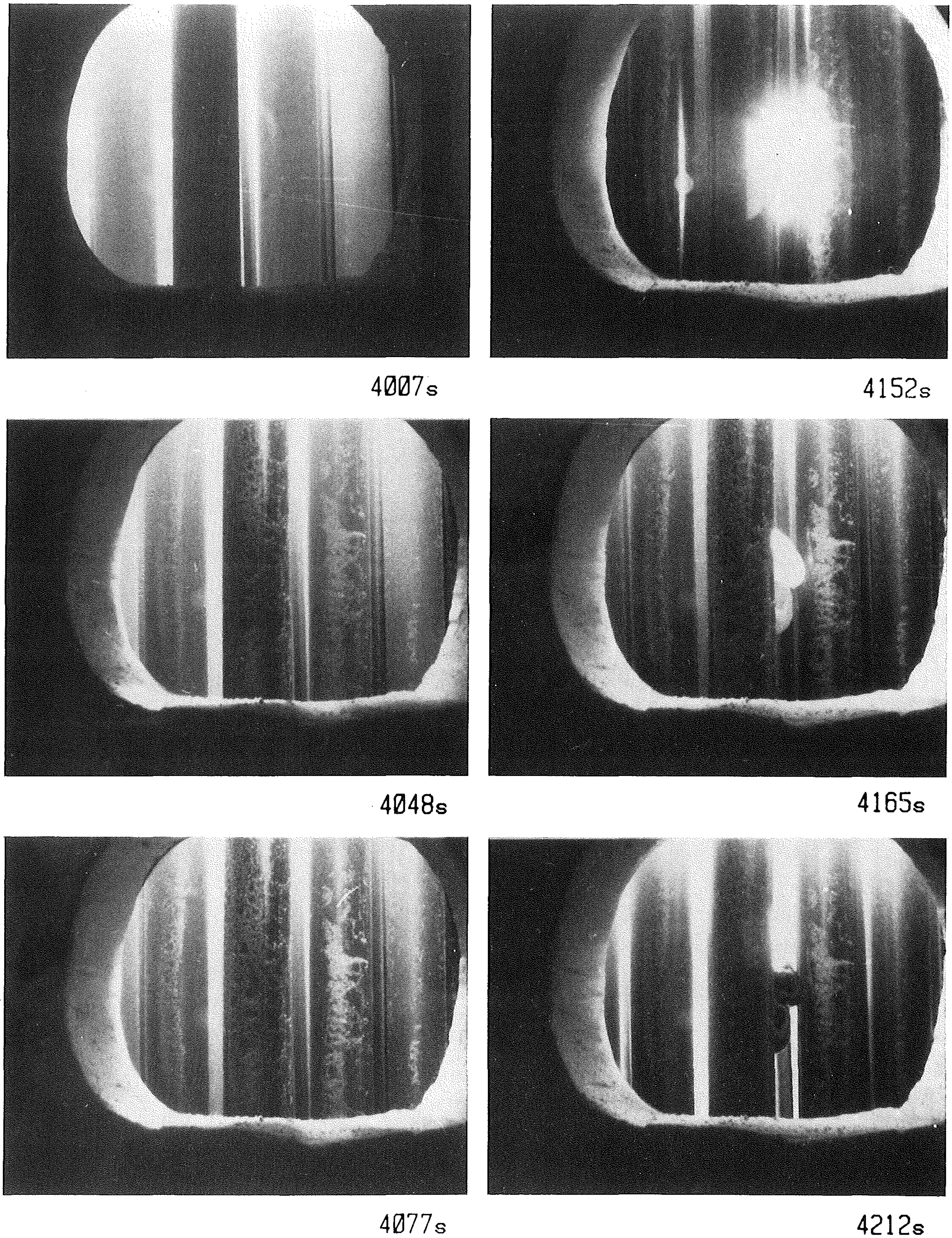

<u>Fig. 5:</u> **Videoscope pictures of fuel rod simulators 36, 43, 38, 32 taken at <u>300 mm elevation</u>, 300°, H26; (transient test CORA-C)**

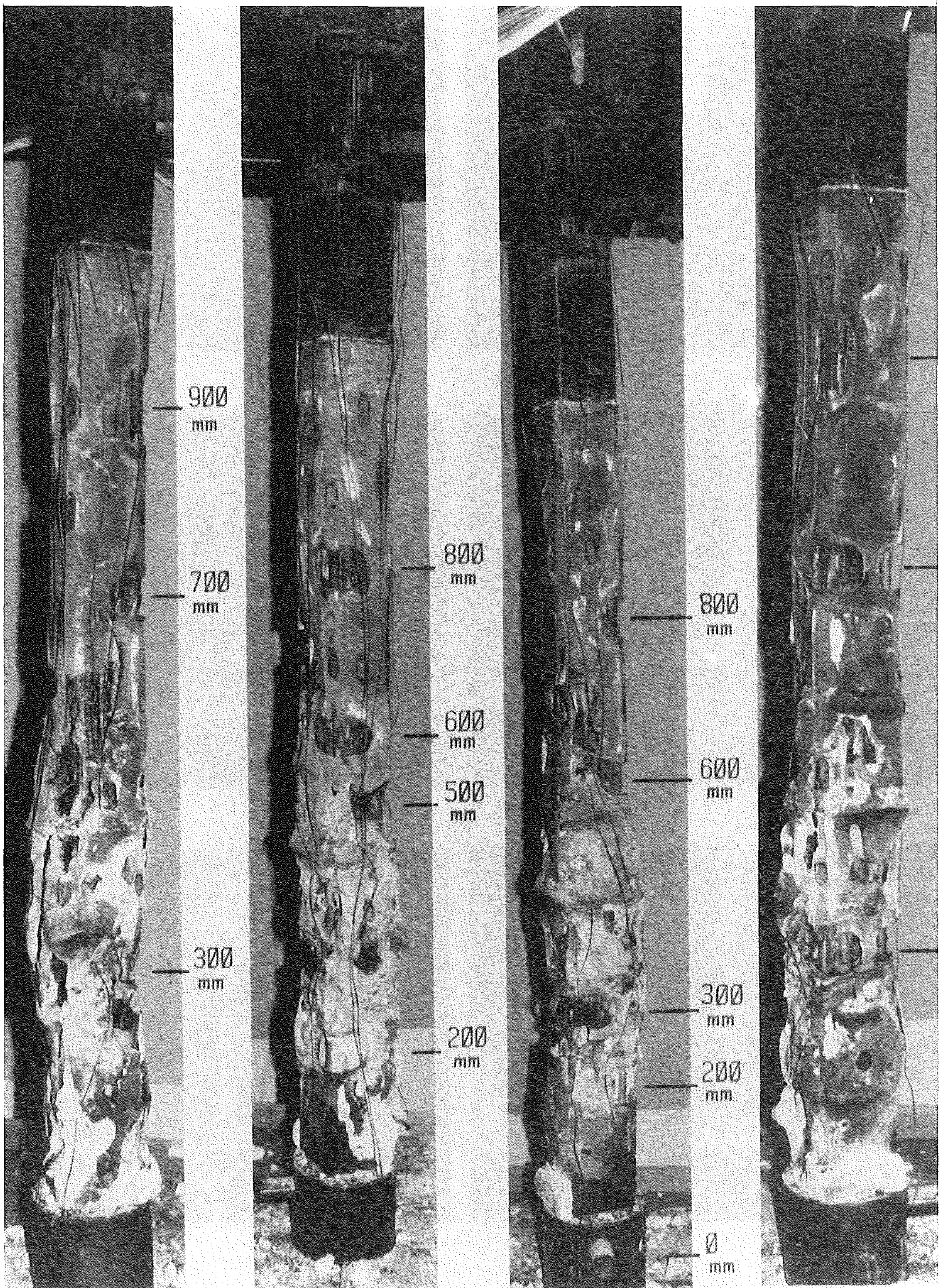

<u>Fig. 6:</u> **Post-test appearance of CORA-bundle C after removal of shroud insulation**

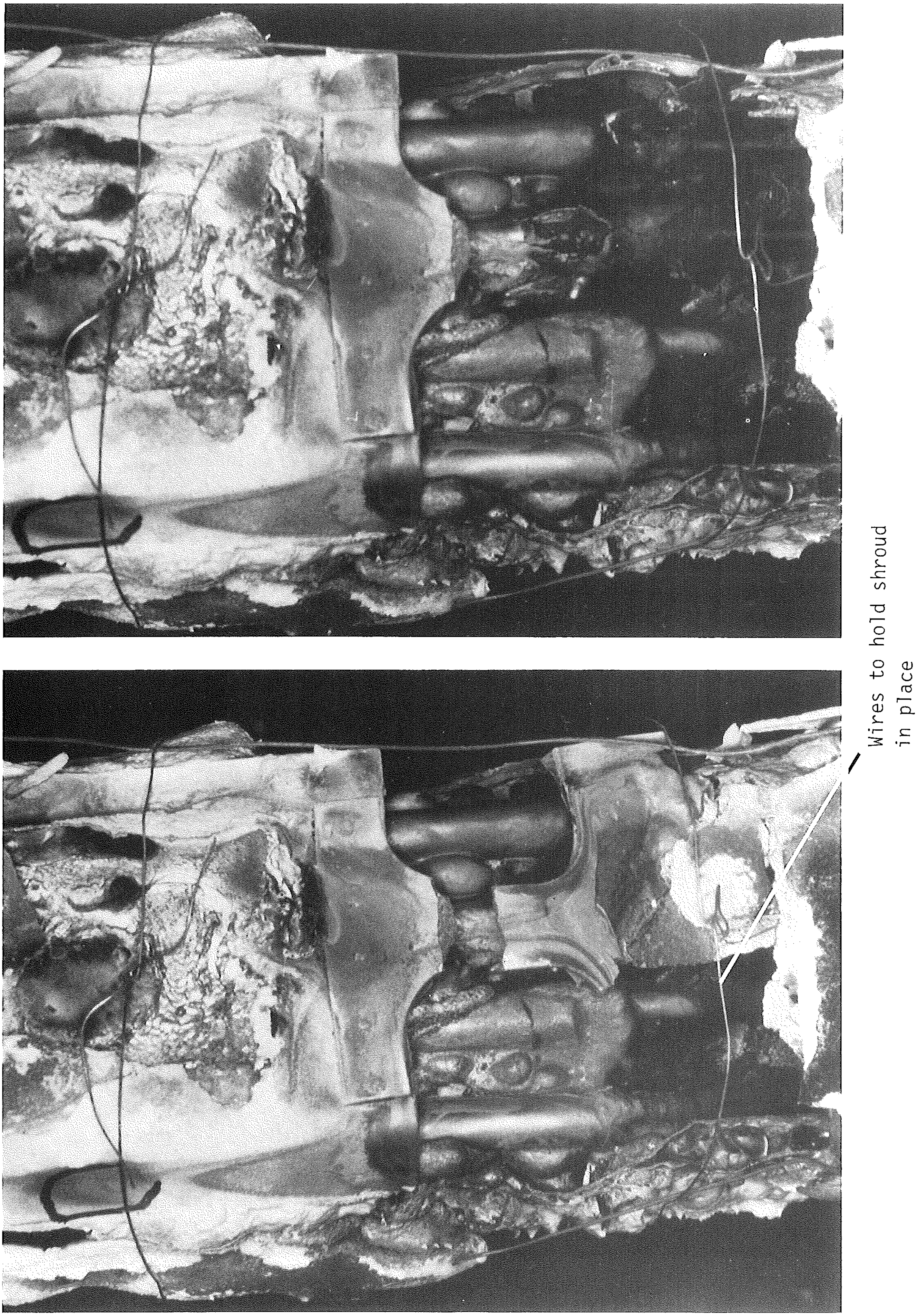

Fig. 7: **Details of CORA bundle C at 250 mm to 430 mm elevation (260°)**

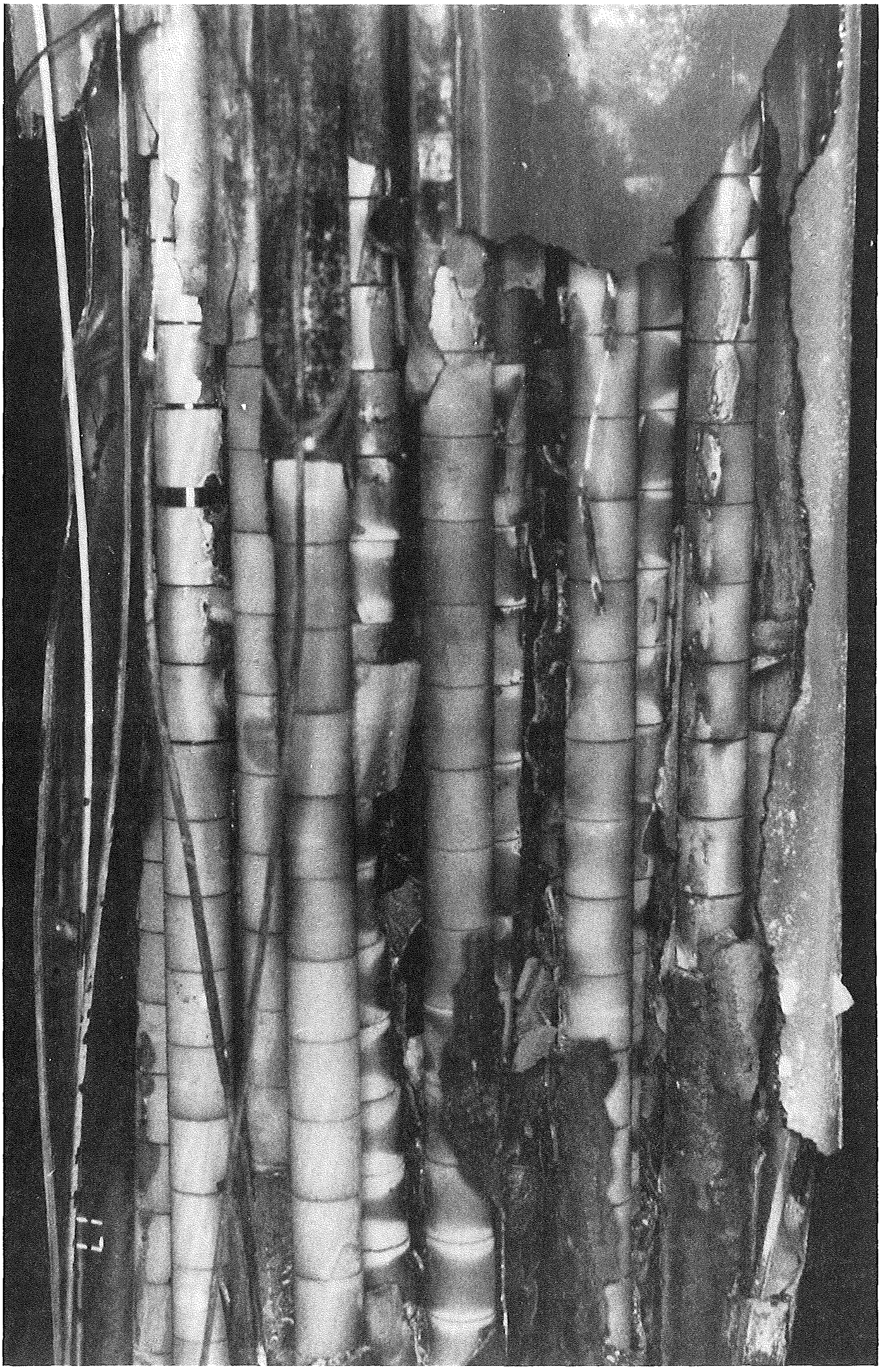

Fig. 8: Details of CORA bundle C at 770 mm to 930 mm elevation (290°)

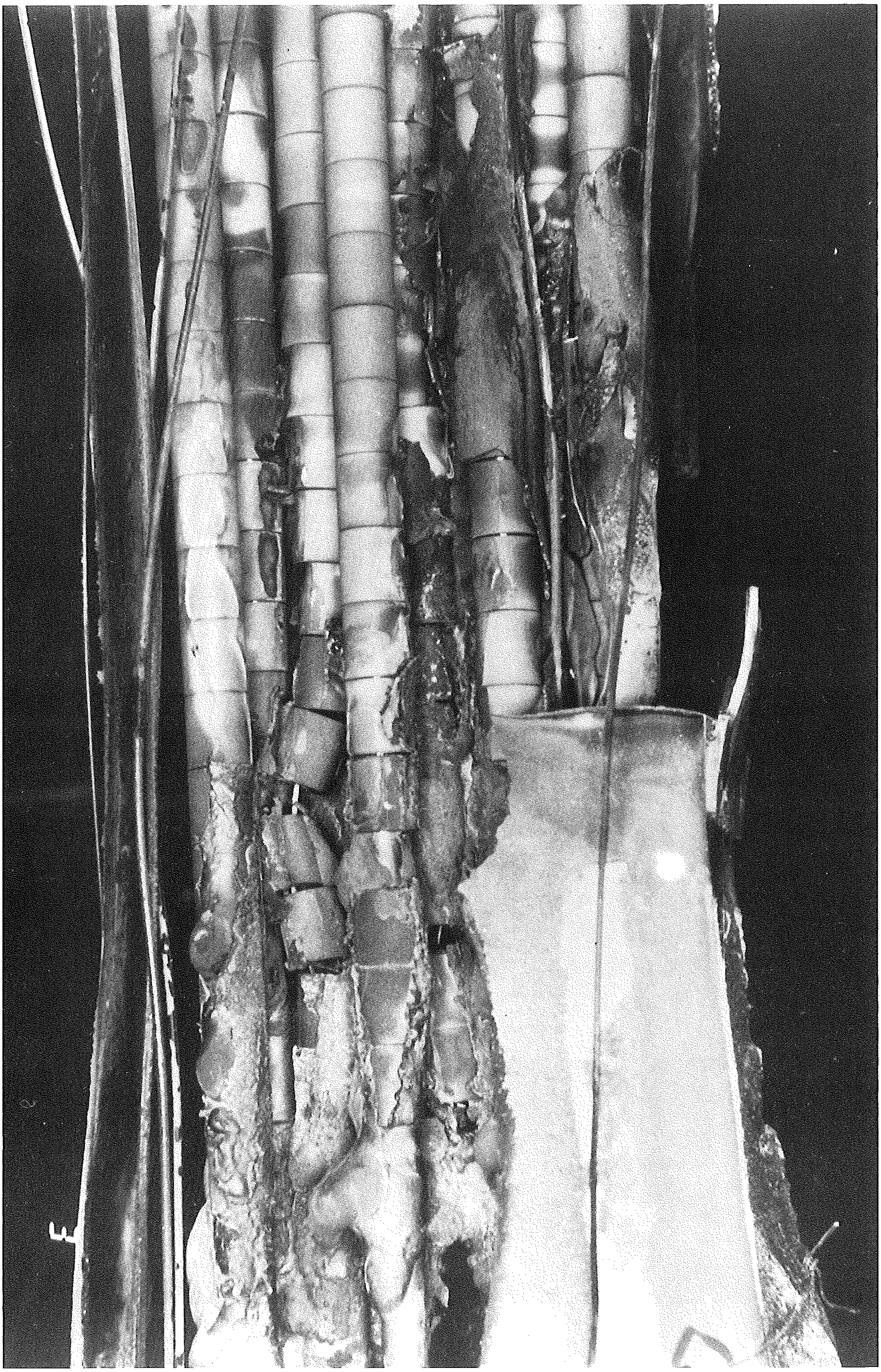

Fig. 9: Details of CORA bundle C at 610 mm to 800 mm elevation (340°)

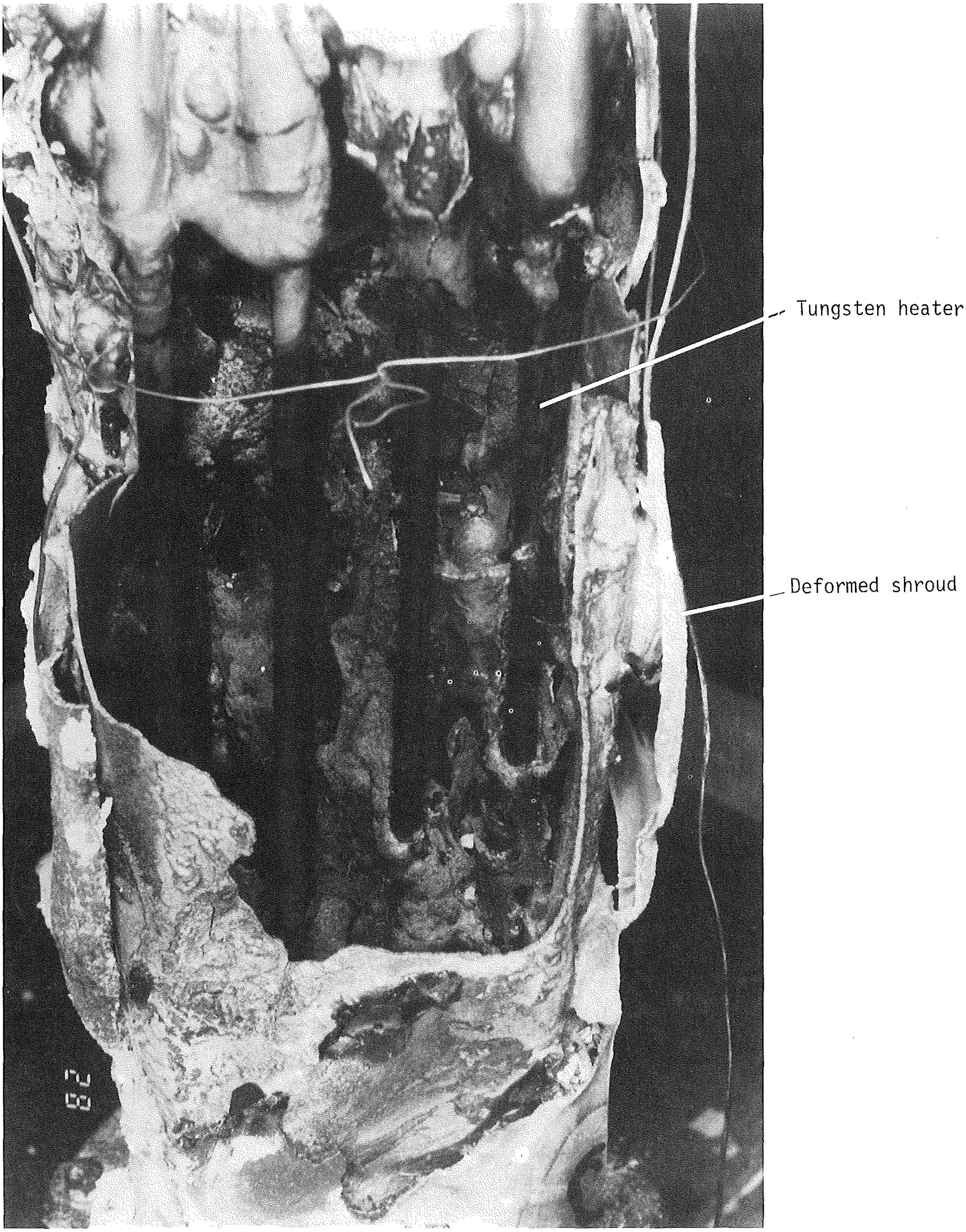

Fig. 10: **CORA bundle C after removal of shroud above 100 mm elevation**

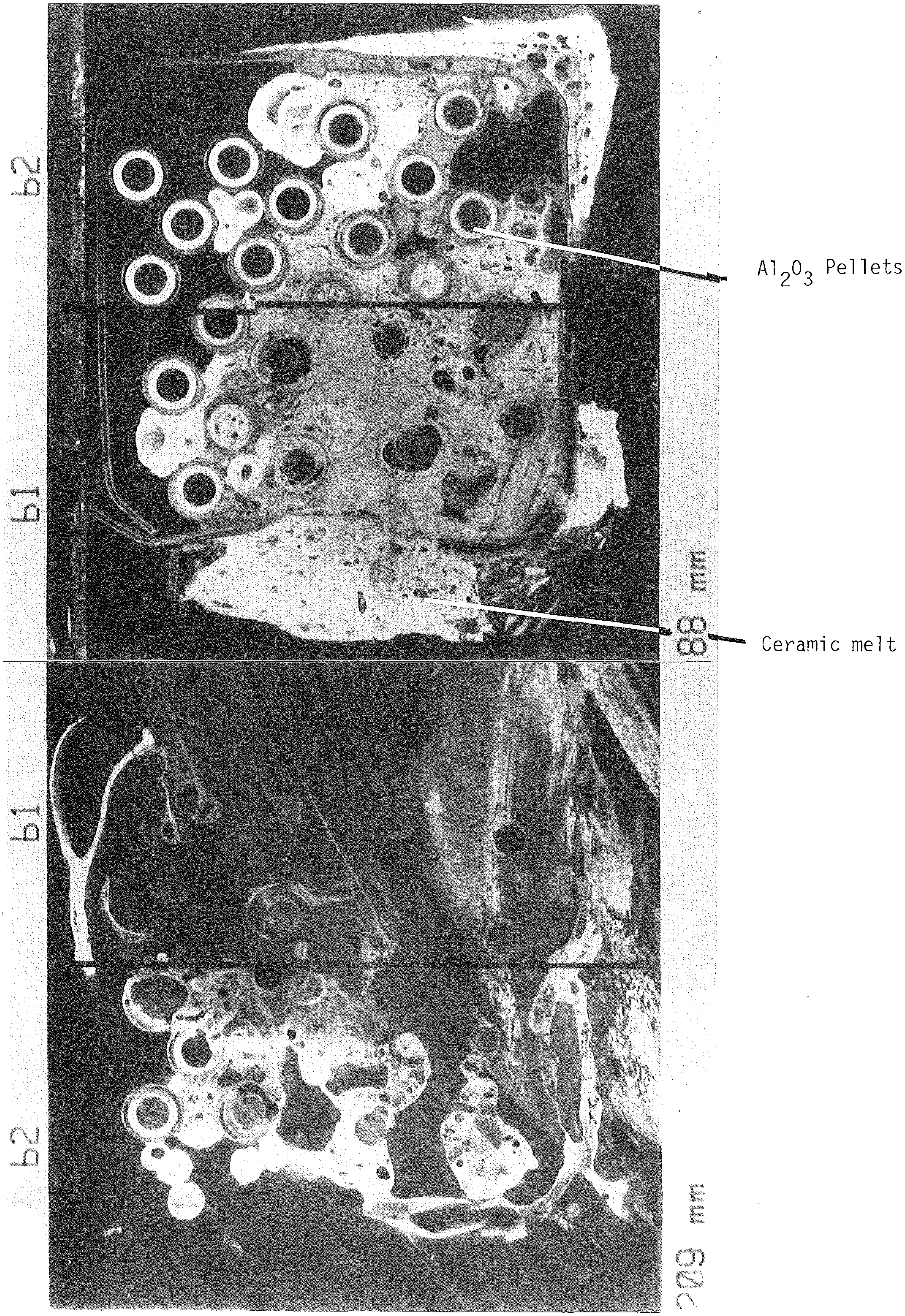

Fig. 11: Horizontal cross sections at 88 mm and 209 mm showing the position of the vertical cross sections b1 and b2 (CORA C)

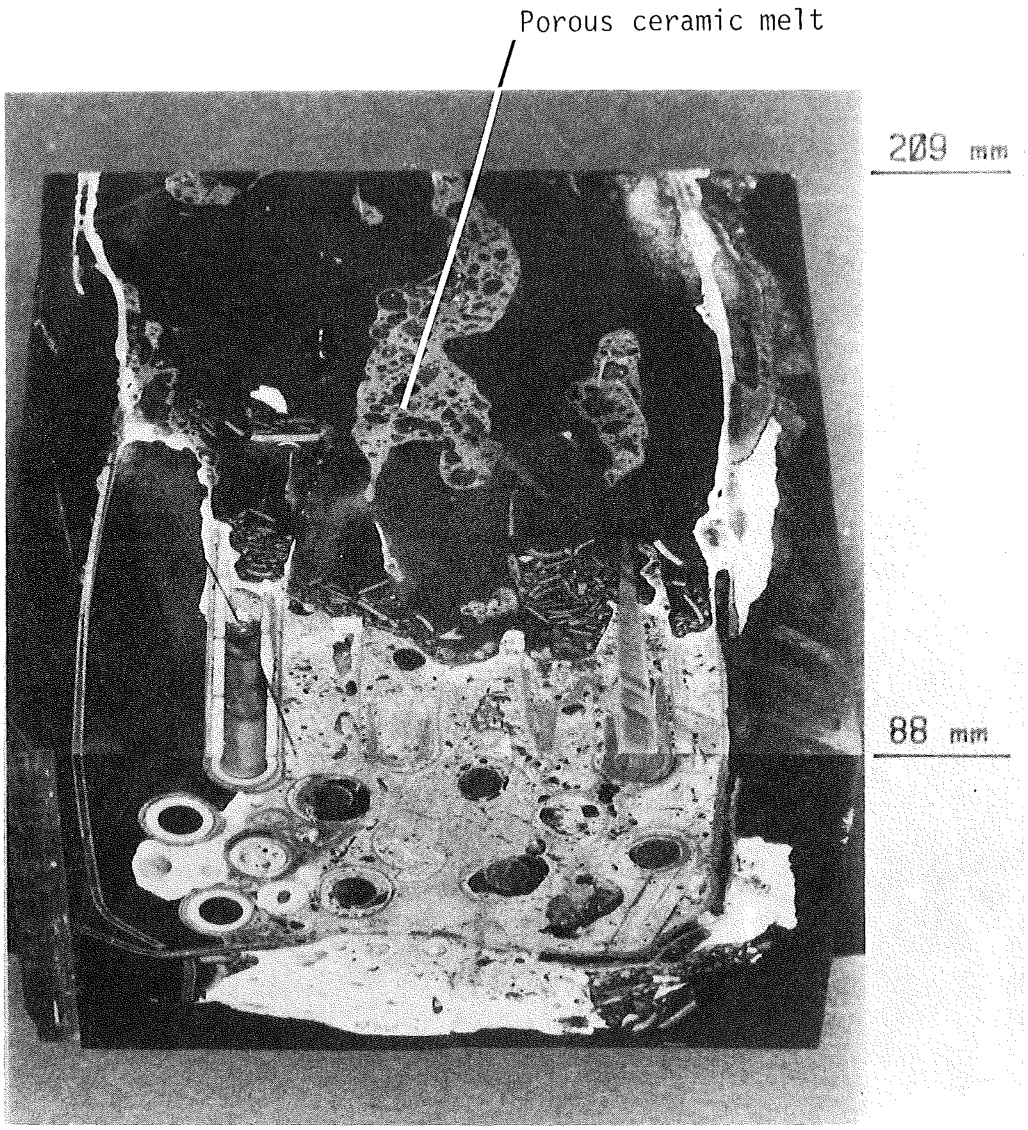

Fig. 12: **Longitudinal section b2 of bundle CORA-C between 88 mm and 209 mm elevation**

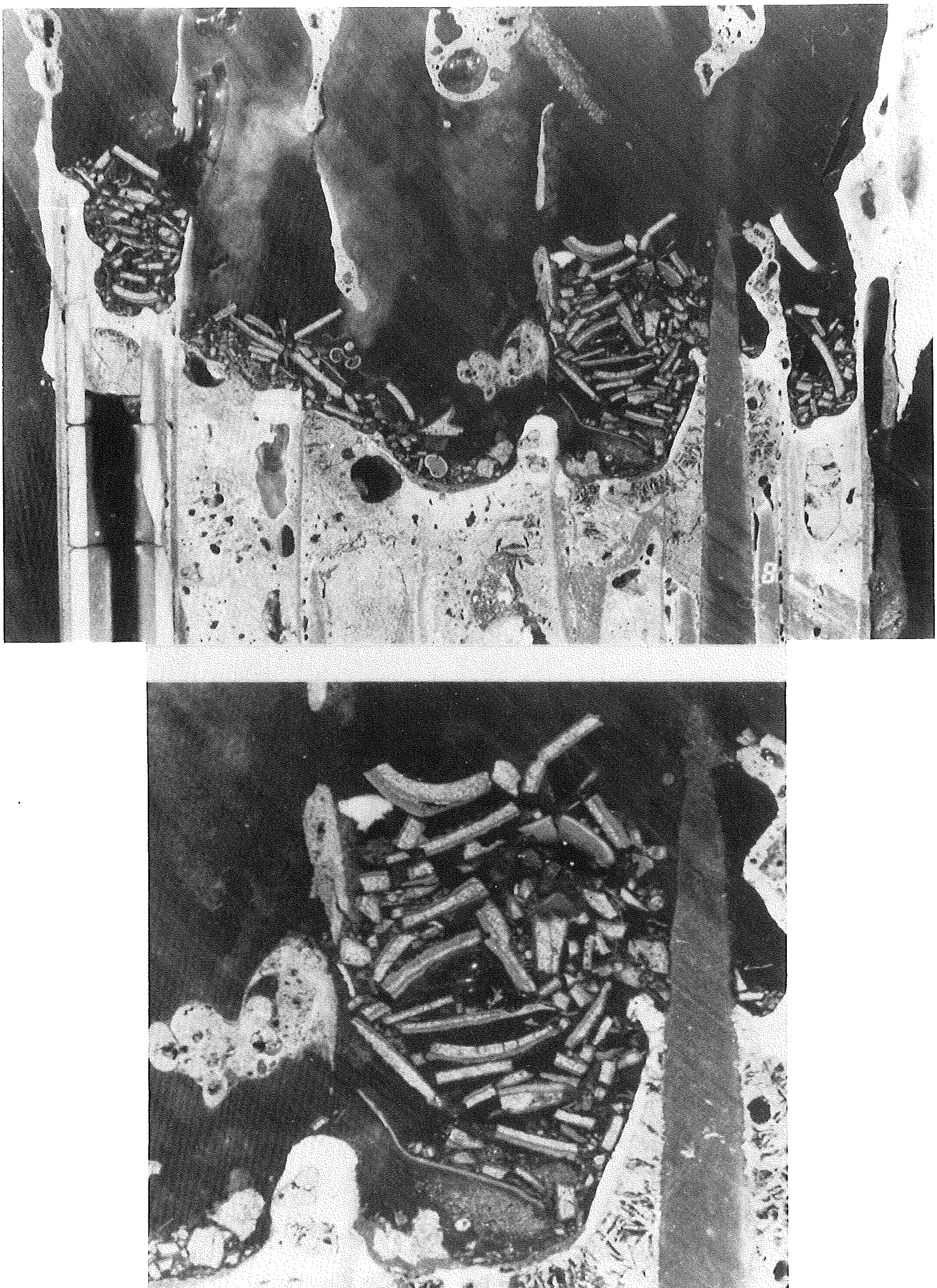

Fig. 13: **Details of vertical cross section b1 between 88 mm and 209 mm elevation (CORA-C)**

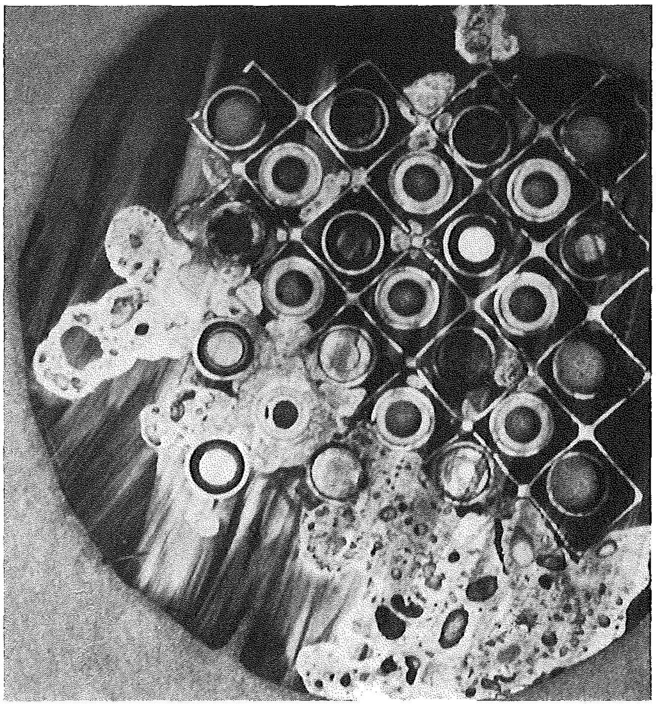

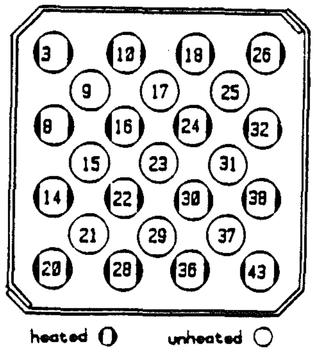

-4 mm

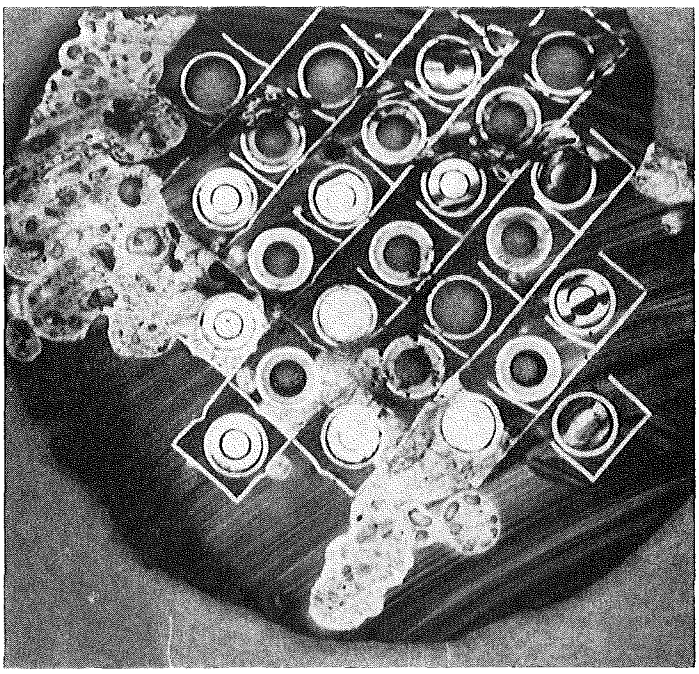

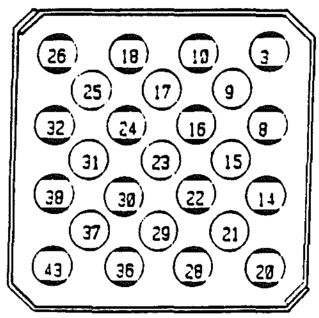

-17 mm

Fig. 14: Cross sections of bundle CORA-C at elevations of the lower grid spacer

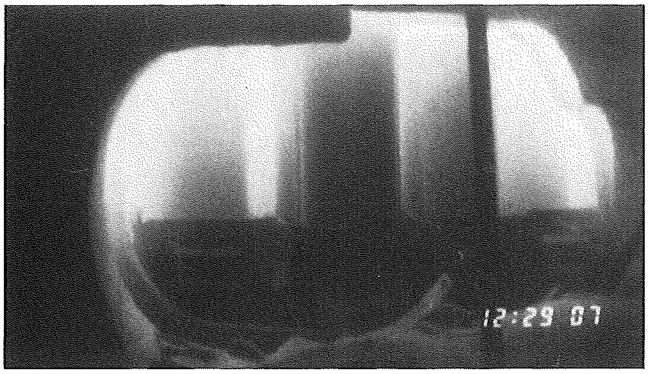

4147 sec

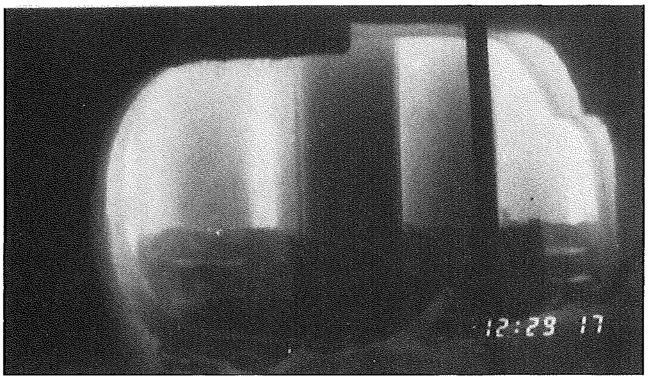

4157 sec

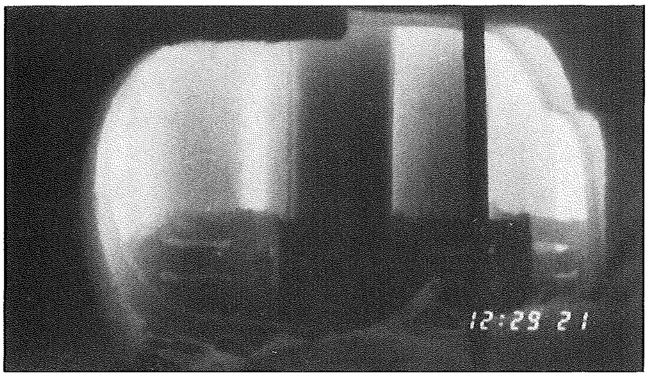

4161 sec

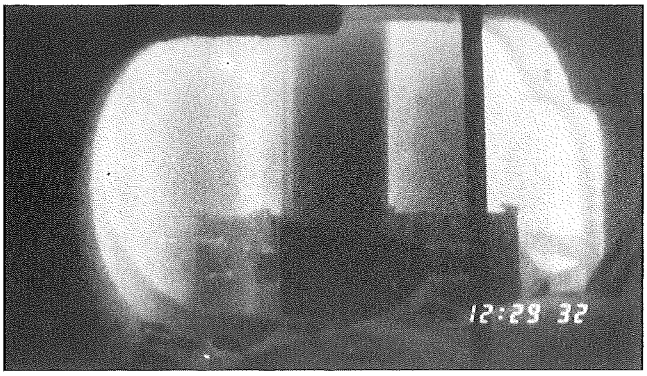

4172 sec

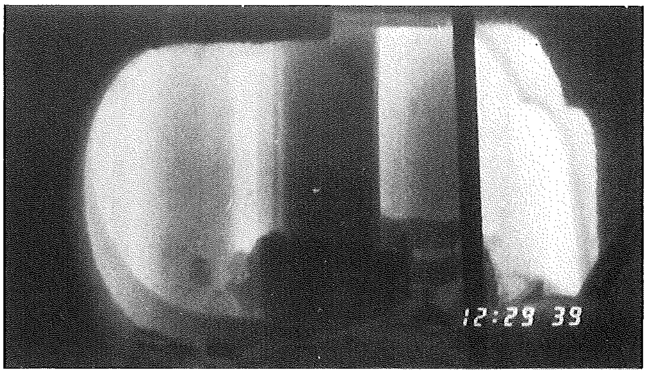

4179 sec

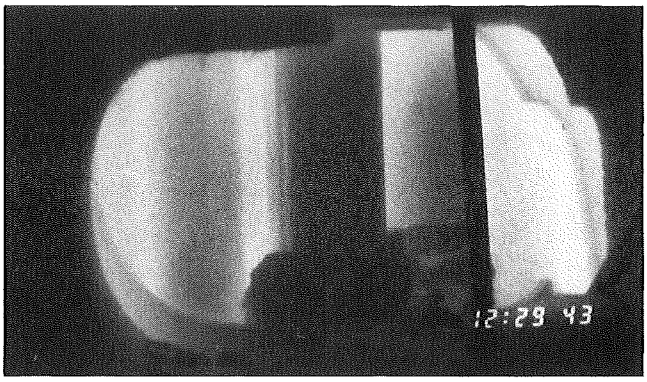

4183 sec

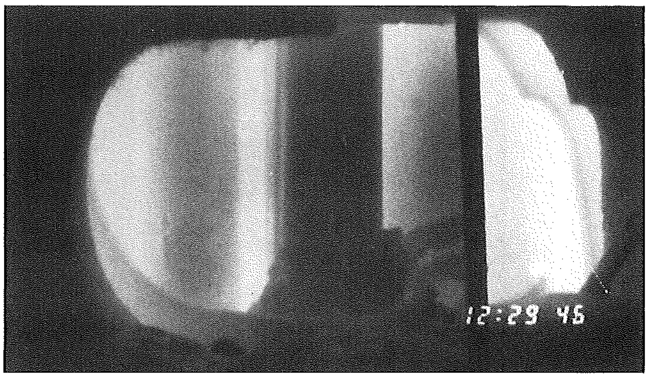

4186 sec

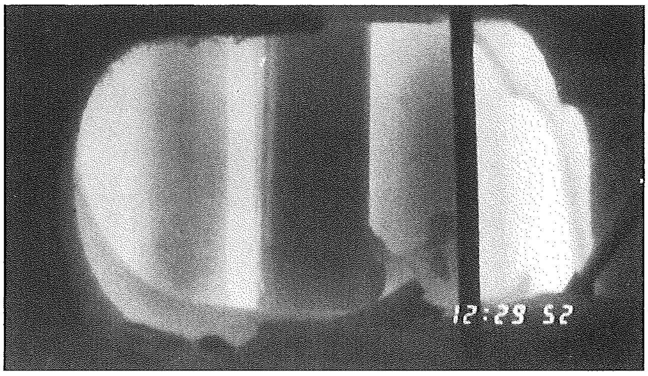

4192 sec

Fig. 15: **Melting of Inconel spacer seen by videoscope at 500 mm elevation (CORA-2)**

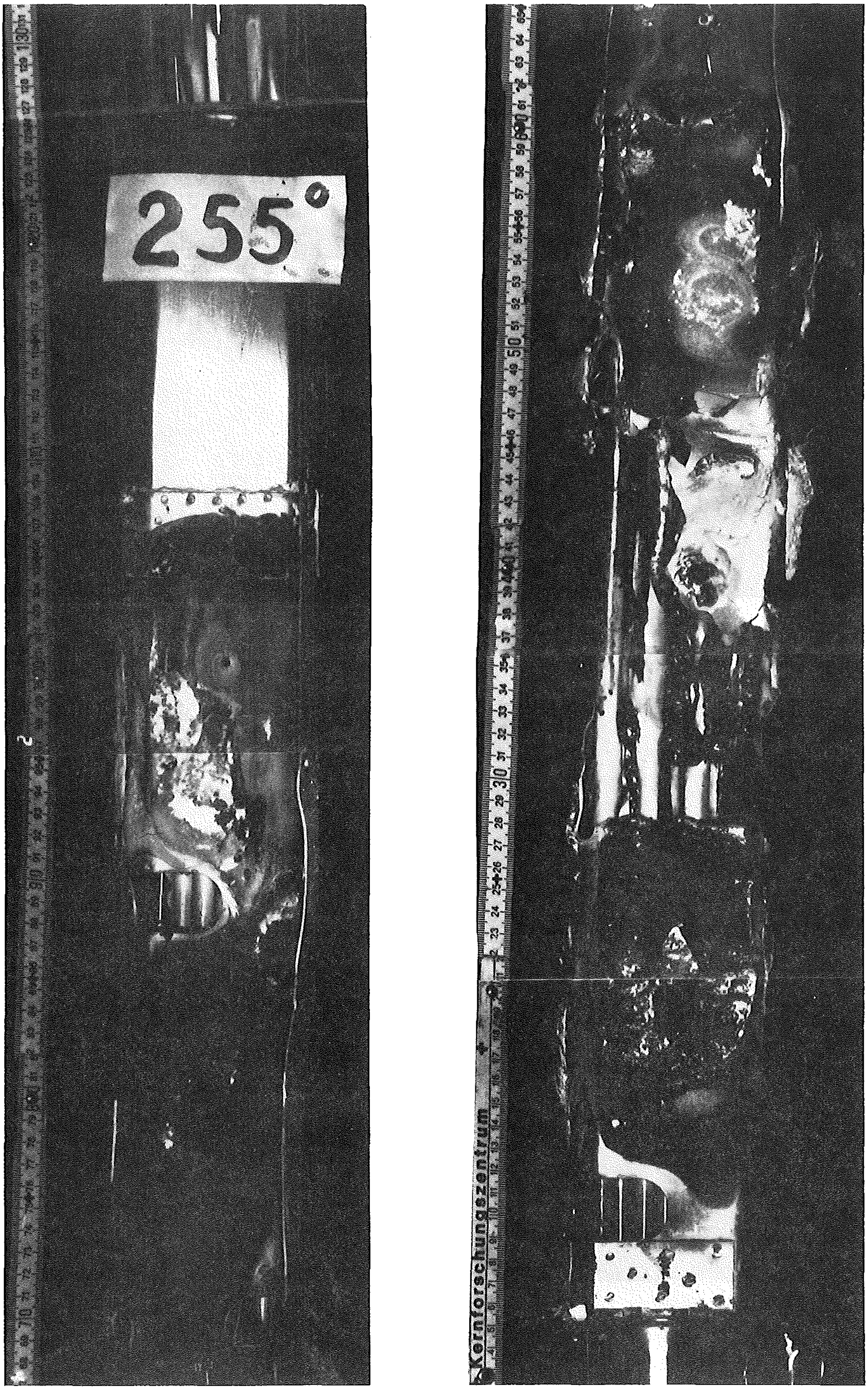

Fig. 16: **Post-test appearance of CORA-2**

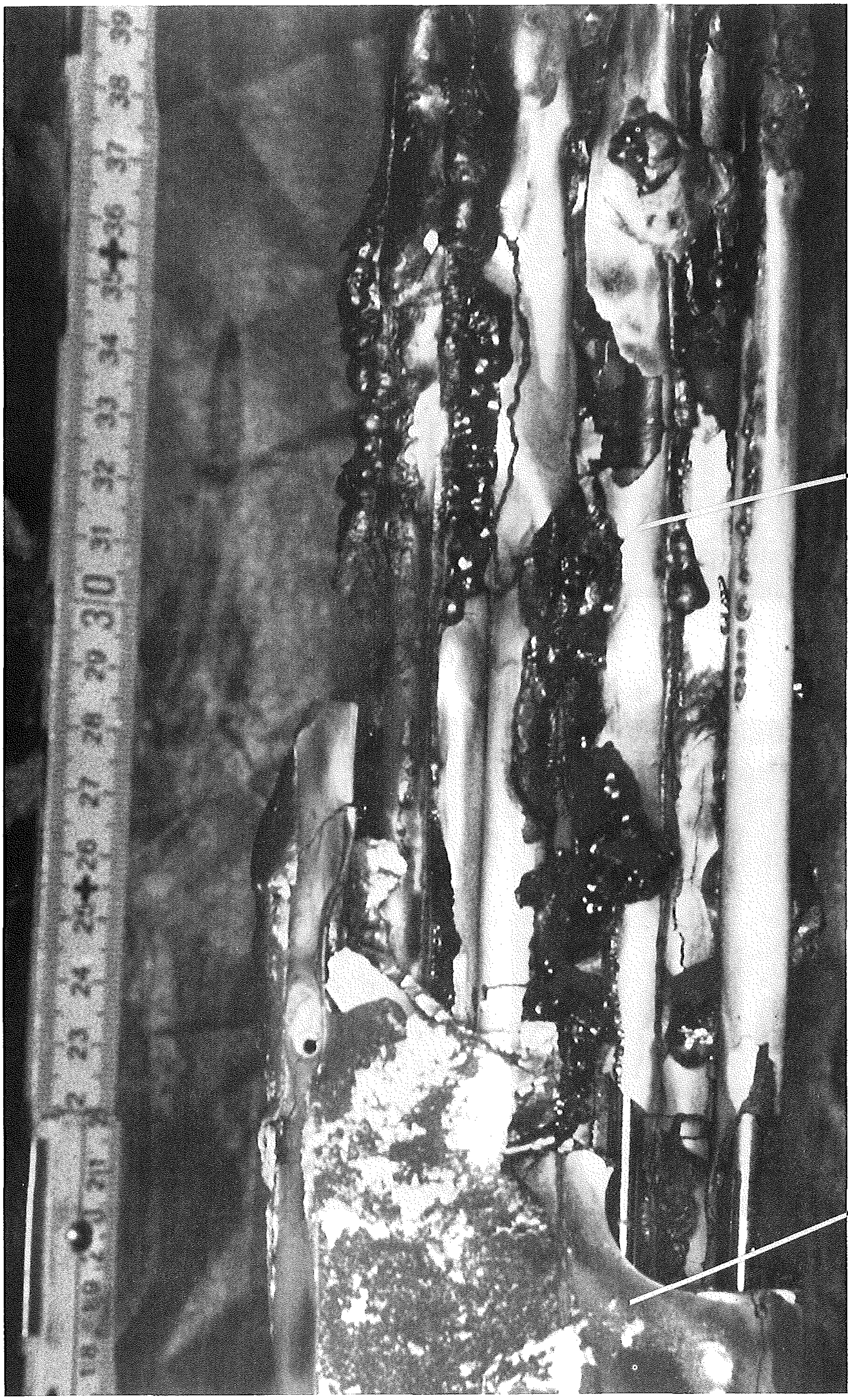

Fig. 17: **Lower end of bundle CORA-2, shroud removed**

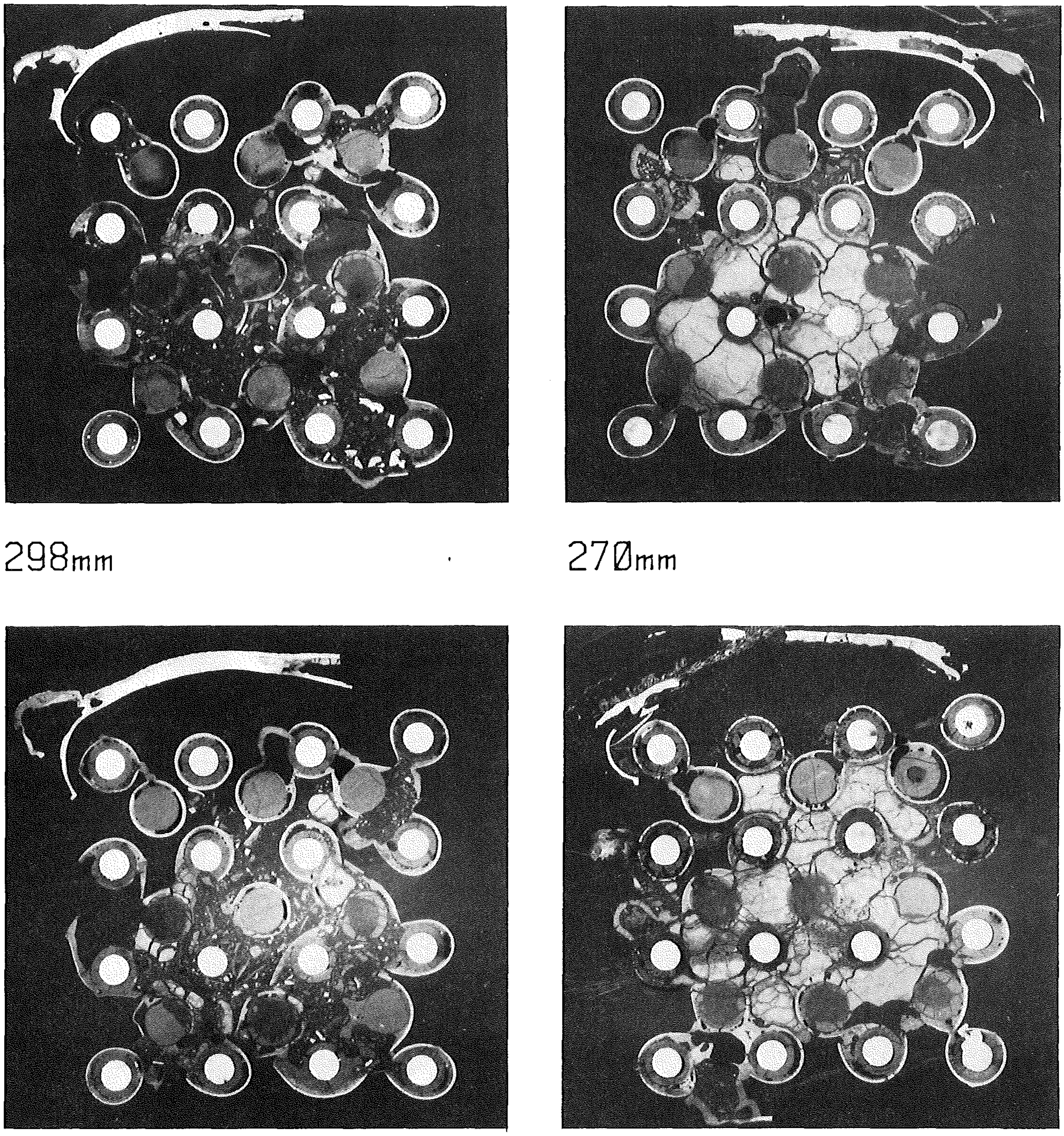

298mm

270mm

283mm

253mm

Fig. 18: **Cross sections CORA-2 at elevation given**

CORA-2

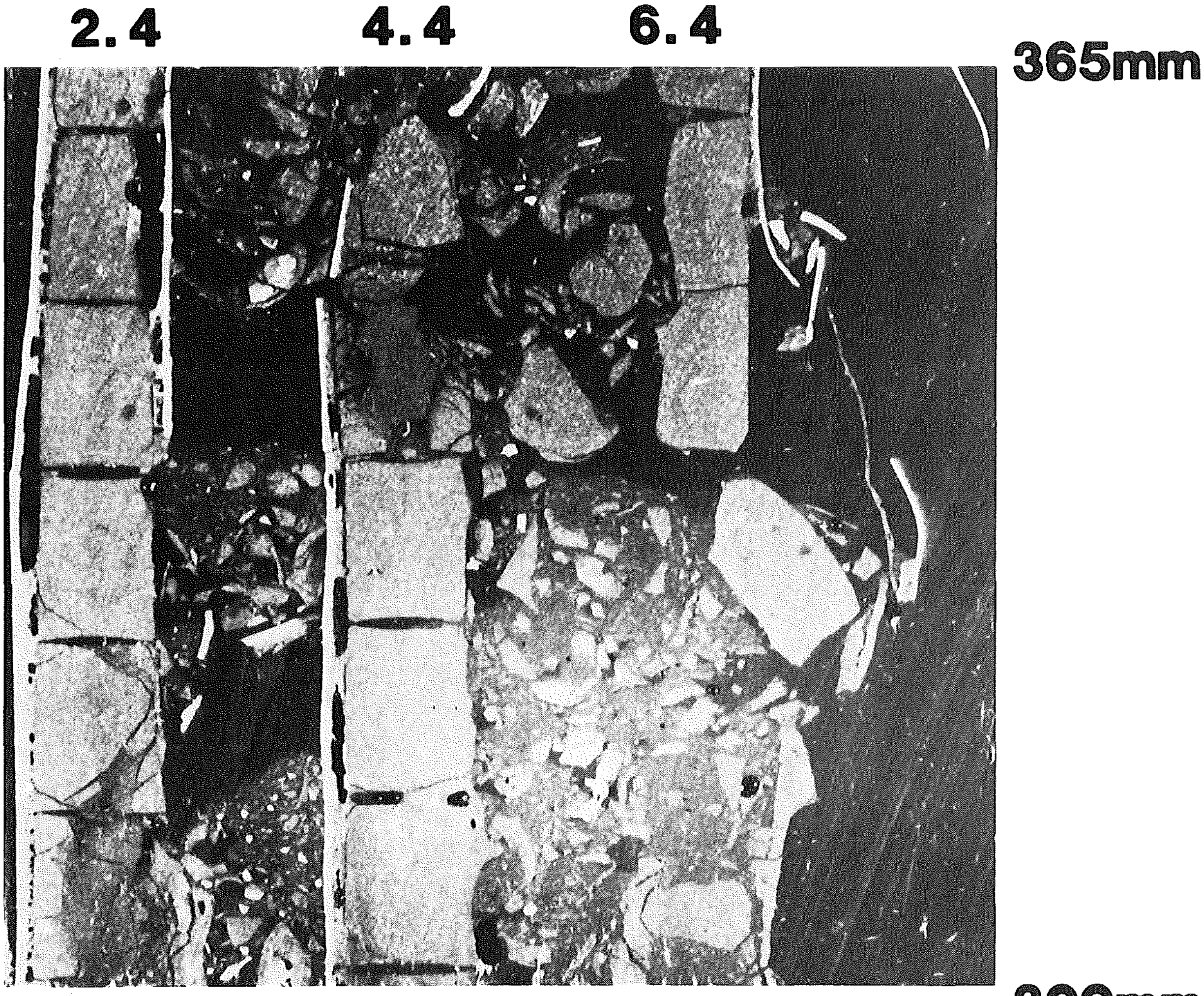

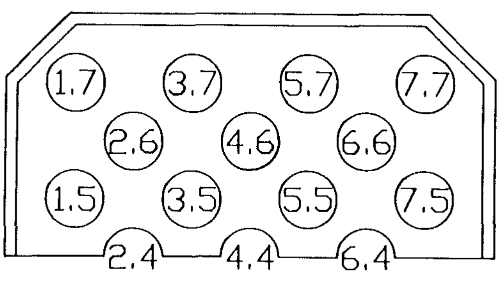

Fig. 19: Longitudinal section of test bundle CORA-2

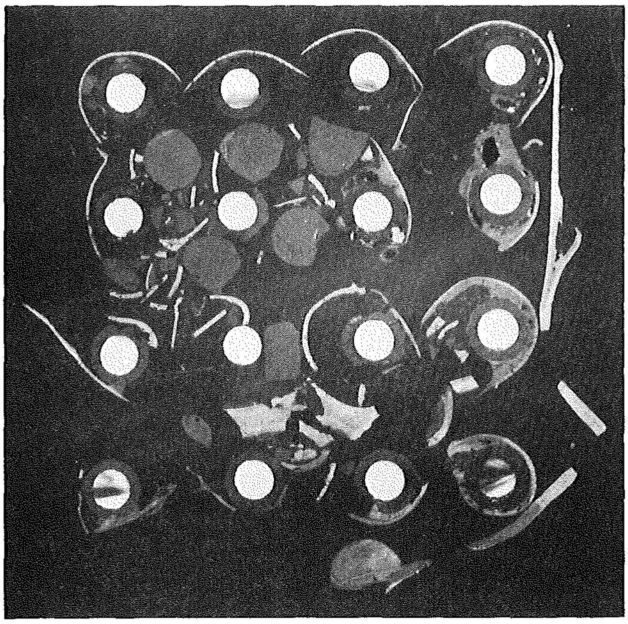

510mm

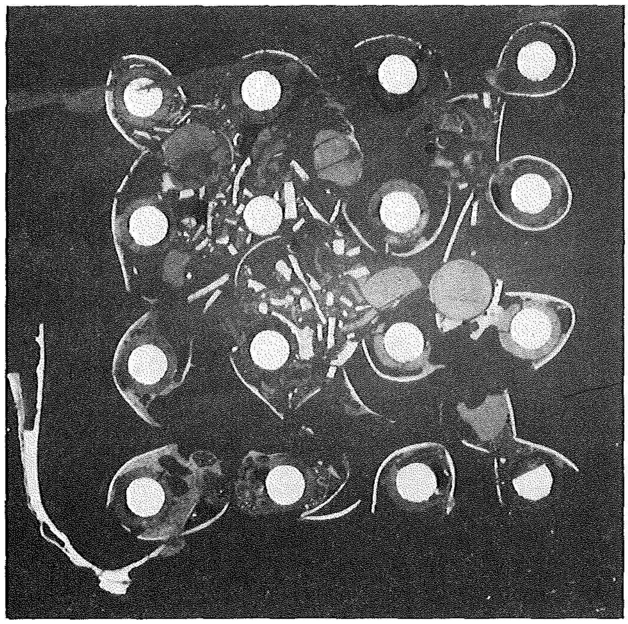

435mm

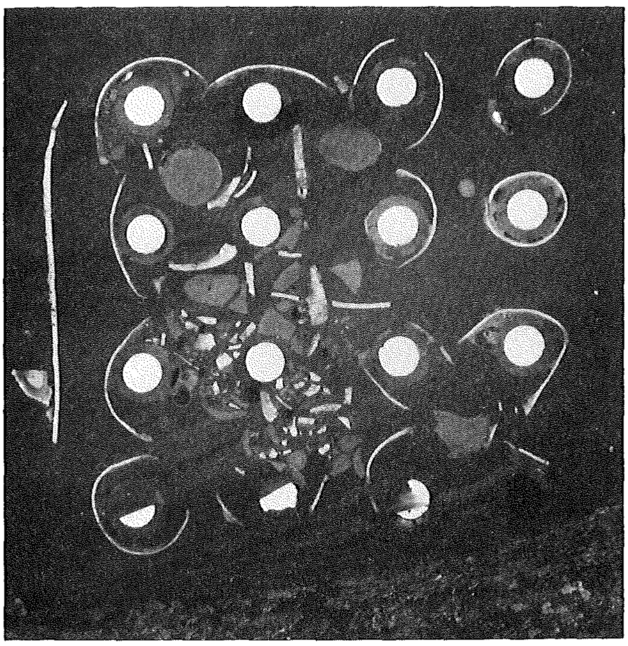

465mm

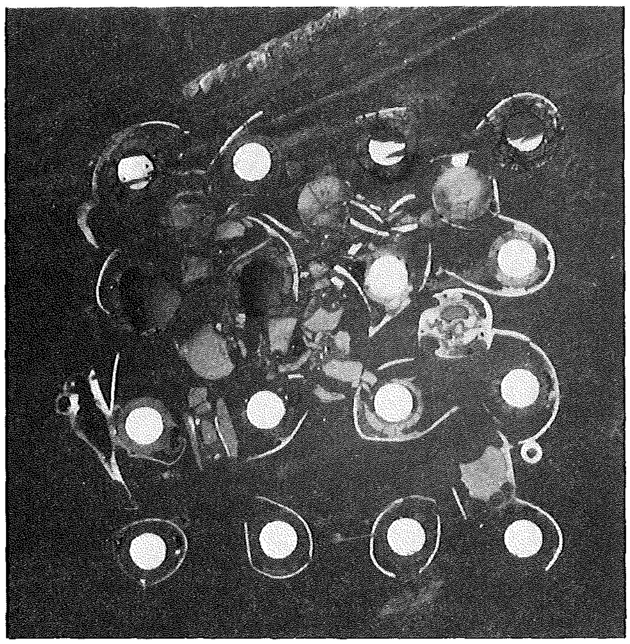

380mm

Fig. 20: **Cross sections of the central region of bundle CORA-2**

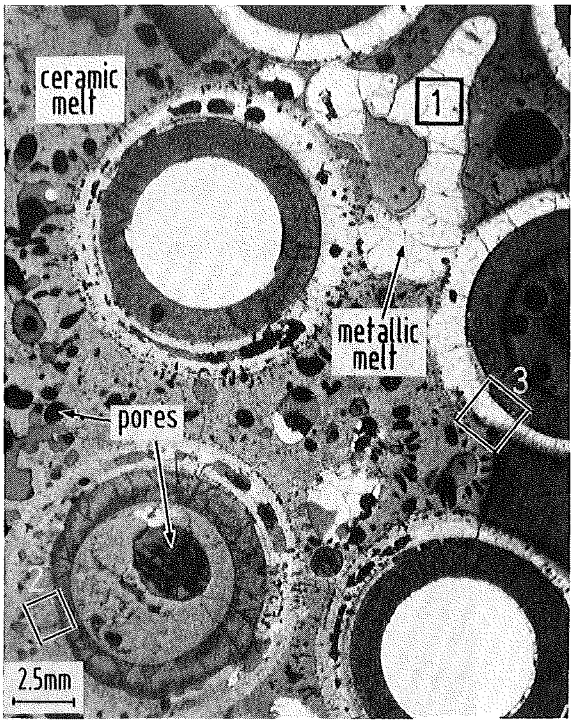

detail of cross-section C 7 (71mm)

position 1

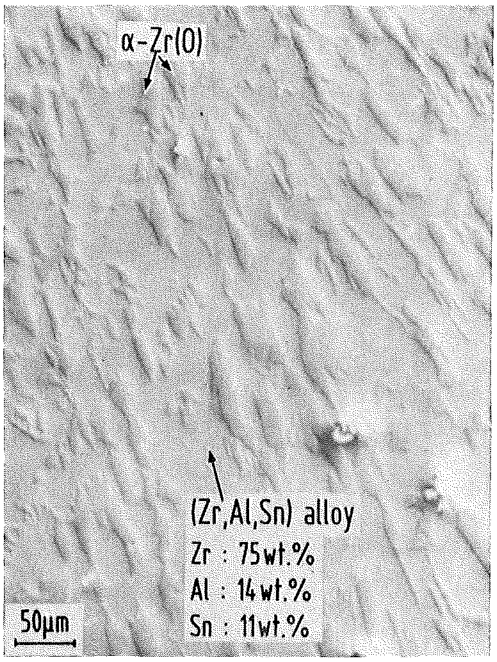

Al/Zr eutectic

position 2

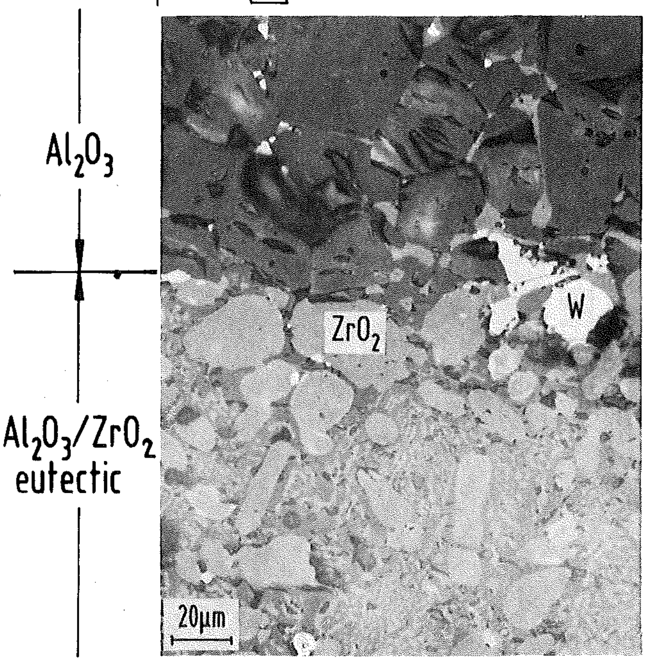

attack of Al_2O_3 pellet

position 3

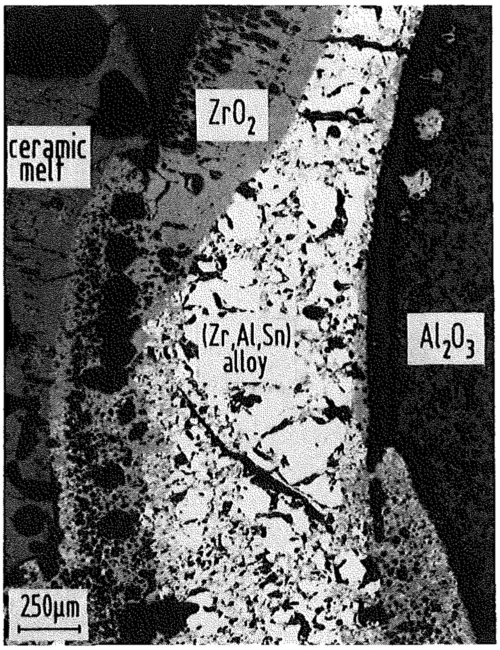

molten Zry/Al_2O_3 interaction

Fig. 21: **Microstructures of CORA bundle cross section C7 (71 mm)**

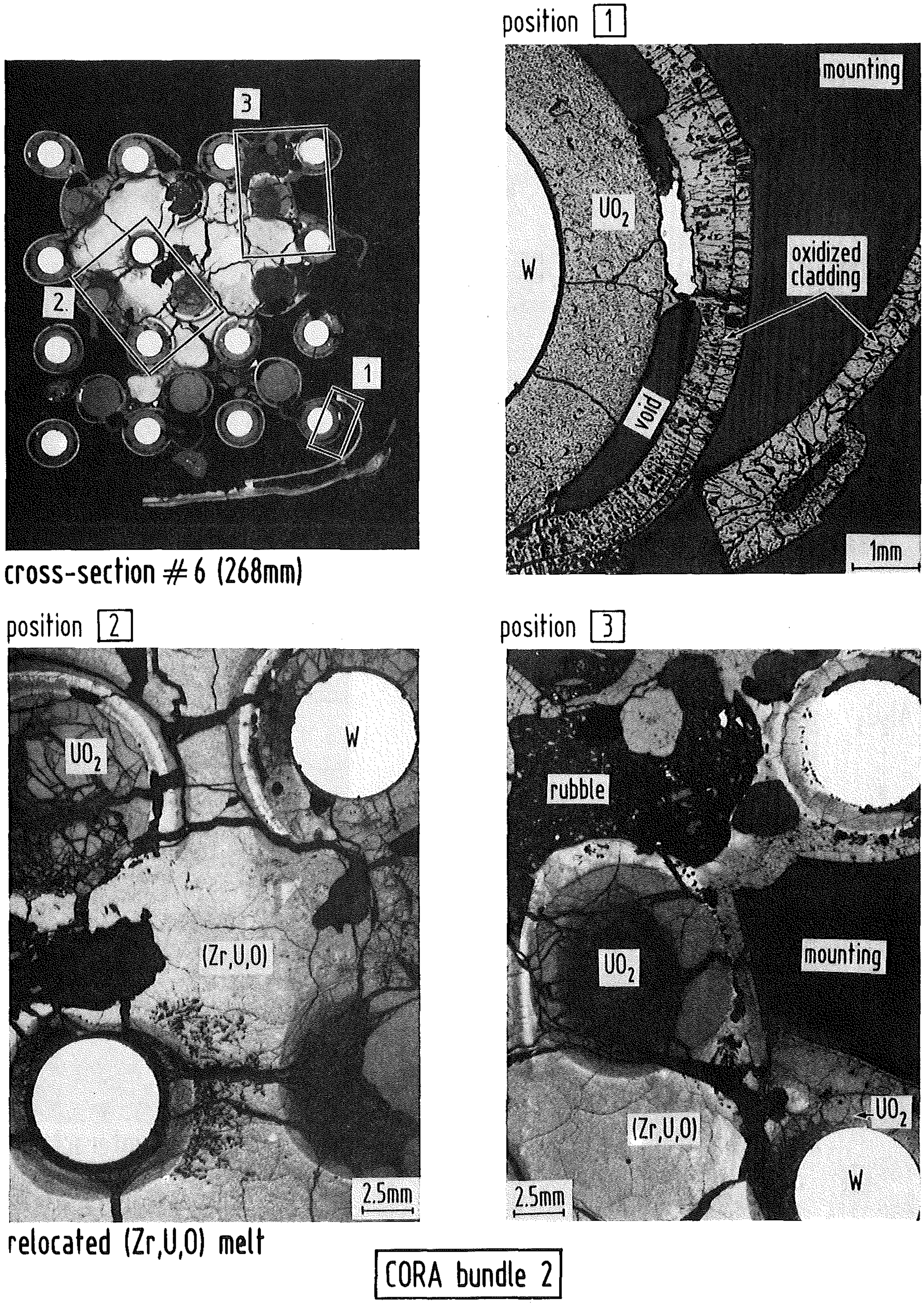

Fig. 22: **CORA-2 bundle cross section #6 (268 mm)**